Supporting Information for

Synthesis and Photophysical Properties of (Post-)Functionalized BOAHY Dyes with Strong Aggregation-Induced Emission

Jonathan B. F. Vandenwijngaerden [a #], Jianjun Huang [b #], Charlotte Cresens [a], Wim Dehaen [b], Luc Van Meervelt [c], Susana Rocha [a], Mark Van der Auweraer [a] and Eduard Fron [a,d]

[a] Molecular Imaging and Photonics, Department of Chemistry, KU Leuven, Celestijnenlaan 200F, 3001 Leuven, Belgium.

[b] Sustainable Chemistry for Metals and Molecules, Department of Chemistry, KU Leuven, Celestijnenlaan 200F, 3001 Leuven, Belgium.

[b] Biochemistry, Molecular and Structural Biology, Department of Chemistry, KU Leuven, Celestijnenlaan 200F, 3001 Leuven, Belgium.

[d] KU Leuven Core Facility for Advanced Spectroscopy, Celestijnenlaan 200F, 3001 Leuven, Belgium.

[#] J.B.F.V. and J.H. are joint first authors

To whom all correspondence should be addressed: eduard.fron@kuleuven.be

Table of Contents

1. Synthesis Procedures 3
2. Characterization Procedures 9
3. X-Ray Crystallography 12
4. Steady-State Spectroscopy 23
   4.1. Photophysical Properties 23
   4.2. Aggregation in Water/Acetonitrile Mixtures 27
5. Time-Resolved Spectroscopy 37
   5.1. Time-Correlated Single Photon Counting 37
   5.2. Femtosecond Fluorescence Up-Conversion 39
6. Fluorescence Microscopy 41
7. NMR Spectroscopy 43
References 57

1. Synthesis Procedures

General Synthesis Procedure for BOAHY 2a-2d

A mixture of 2-formyl pyrrole (1 mmol) and carbohydrazide (1.1 mmol) in 10 mL ethanol was refluxed after the addition of 3 drops of glacial acetic acid. Reaction was monitored by TLC, and after complete consumption of 2-formyl pyrrole, the solvent was completely evaporated under vacuum. The residue was dissolved in 10 mL dry dichloroethane (for **2a**) or dry toluene (for **2b**-**2d**), followed by adding triethylamine (0.5 mL) and the reaction mixture was stirred for 10 minutes at 0 °C. $BF_3{\cdot}Et_2O$ (1.0 mL) was then added dropwise and the mixture refluxed under argon atmosphere. The cooled reaction mixture was quenched with water and extracted with dichloromethane (DCM). The organic layers were combined and washed with water, dried over magnesium sulfate and concentrated under reduced pressure. The residue was then purified by column chromatography (silica gel) using petroleum ether and DCM as eluent to afford the corresponding BOAHY as pure solids. The compound was then further purified by recrystallization from a DCM/pentane solvent mixture.

Synthesis of BOAHY 2a

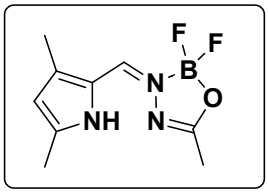

2a

The reaction was performed according to the general procedure with 3,5-dimethyl-1H-pyrrole-2-carbaldehyde (123 mg, 1 mmol) and acetohydrazide (82 mg, 1.1 mmol) to afford the intermediate hydrazone, after simple concentration of the reaction mixture under vacuum, followed by addition of 10 mL dry dichloroethane, triethylamine (0.5 mL) after which the reaction mixture was stirred for 10 minutes at 0 °C. $BF_3{\cdot}Et_2O$ (1.0 mL) was then added dropwise and the mixture refluxed under nitrogen for 3h to afford the desired product **2a**.

Yield: 55%, mp: 215 – 216 °C.

^{1}H NMR (400 MHz, $CDCl_3$) δ 10.70 (bs, 1H), 7.44 (s, 1H), 6.02 – 5.98 (m, 1H), 2.38 (s, 3H), 2.26 (s, 3H), 2.20 (s, 3H); ^{13}C NMR (101 MHz, $CDCl_3$) δ 171.65, 141.68, 138.54, 134.80, 121.59, 113.71, 16.02, 14.04, 11.37; ^{11}B NMR (128 MHz, $CDCl_3$) δ 4.06 (t, J = 17.6 Hz); ^{19}F NMR (376 MHz, $CDCl_3$) δ -150.35 (dd, J = 35.0, 16.7 Hz).

HRMS (ESI, $[M + H]^+$) for $C_9H_{13}BF_2N_3O$ calcd 228.1114, found 228.1118.

Synthesis of BOAHY 2b

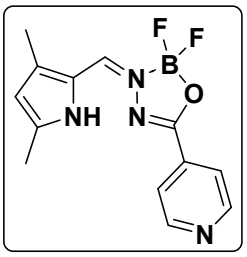

2b

To a round-bottom flask equipped with a magnetic stirring bar, 3,5-dimethyl-1H-pyrrole-2-carbaldehyde (123 mg, 1 mmol) and pyridine-4-carbohydrazide (151 mg, 1.1 mmol) were combined to afford the intermediate hydrazone, after simple concentration of the reaction mixture under vacuum, followed by addition of 10 mL dry toluene, triethylamine (0.5 mL) after which the reaction mixture was stirred for 10 minutes at 0 °C. $BF_3{\cdot}Et_2O$ (1.0 mL) was then added dropwise and the mixture refluxed under nitrogen for 3h to afford the desired product **2b**.

Yield: 80%; mp: 241 – 242 °C.

^{1}H NMR (400 MHz, $CDCl_3$) δ 10.63 (bs, 1H), 8.75 (dd, *J* = 4.5, 1.6 Hz, 2H), 7.78 (dd, *J* = 4.5, 1.6 Hz, 2H), 7.41 (s, 1H), 6.06 (d, *J* = 2.5 Hz, 1H), 2.48 (s, 3H), 2.20 (s, 3H); ^{13}C NMR (101 MHz, $CDCl_3$) δ 166.08, 150.60, 144.10, 140.67, 135.59, 134.81, 121.87, 121.30, 114.51, 14.35, 11.46; ^{11}B NMR (128 MHz, $CDCl_3$) δ 4.37 (t, *J* = 16.3 Hz); ^{19}F NMR (377 MHz, $CDCl_3$) δ -148.38 (dd, *J* = 33.0, 11.6 Hz).

HRMS (ESI, $[M + H]^+$) for $C_{13}H_{14}BF_2N_4O$ calcd 291.1223; found 291.1218.

Synthesis of BOAHY 2c

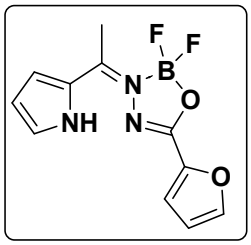

2c

BOAHY **2c** was obtained from the condensation of 2-acetyl-pyrrole (109 mg, 1 mmol) and furan-2-carbohydrazide (139 mg, 1.1 mmol) to afford the intermediate hydrazone, after simple concentration of the reaction mixture under vacuum, followed by addition of 10 mL dry toluene, triethylamine (0.5 mL) after which the reaction mixture was stirred for 10 minutes at 0 °C. $BF_3{\cdot}Et_2O$ (1.0 mL) was then added dropwise and the mixture refluxed under nitrogen for 3h to afford the desired product **2c**.

Yield: 79%; mp: 156 – 157 °C.

^{1}H NMR (400 MHz, $CDCl_3$) δ 11.96 (bs, 1H), 7.68 – 7.62 (m, 1H), 7.35 (t, *J* = 3.2 Hz, 1H), 7.29 – 7.23 (m, 1H), 7.16 – 7.10 (m, 1H), 6.59 (dd, *J* = 3.5, 1.7 Hz, 1H), 6.47 – 6.41 (m, 1H), 2.68 (s, 3H); ^{13}C NMR (101 MHz, $CDCl_3$) δ 160.10, 152.05, 146.67, 142.83, 128.52, 126.24, 122.68, 117.93, 112.55, 112.16, 16.70; ^{11}B NMR (128 MHz, $CDCl_3$) δ 4.39 (t, *J* = 17.7 Hz)；^{19}F NMR (376 MHz, $CDCl_3$) δ -147.38 (dd, *J* = 34.7, 15.4 Hz).

HRMS (ESI, $[M + H]^+$) for $C_{11}H_{11}BF_2N_3O_2$ calcd 266.0907, found 266.0918.

Synthesis of BOAHY 2d

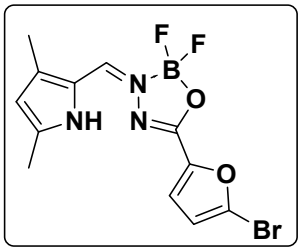

2d

To a round-bottom flask equipped with a magnetic stirring bar, 3,5-dimethyl-1H-pyrrole-2-carbaldehyde (123 mg, 1 mmol) and 5-bromo-2-furohydrazide(226 mg, 1.1 mmol) to afford the intermediate hydrazone, after simple concentration of the reaction mixture under vacuum, followed by addition of 10 mL dry toluene, triethylamine (0.5 mL) after which the reaction mixture was stirred for 10 minutes at 0 °C. $BF_3{\cdot}Et_2O$ (1.0 mL) was then added dropwise and the mixture refluxed under nitrogen for 3h to afford the desired product **2d**.

Yield: 60%; mp: 231 – 233 °C.

^{1}H NMR (400 MHz, $CDCl_3$) δ 10.80 (s, 1H), 7.52 (s, 1H), 7.16 (d, *J* = 3.6 Hz, 1H), 6.52 (d, *J* = 3.6 Hz, 1H), 6.04 (d, *J* = 2.6 Hz, 1H), 2.45 (s, 3H), 2.30 (s, 3H); ^{13}C NMR (101 MHz, $CDCl_3$) δ 159.20, 144.90, 142.88, 139.47, 134.98, 127.56, 122.00, 119.48, 114.53, 114.14, 14.31, 11.51; ^{11}B NMR (128 MHz, $CDCl_3$) δ 4.14 (t, *J* = 16.7 Hz); ^{19}F NMR (377 MHz, $CDCl_3$) δ -149.37 (dd, *J* = 33.5, 14.1 Hz).

HRMS (ESI$[M - H]^-$) for $C_{12}H_{10}B_1F_2N_3OBr$ calcd 356.0023, found 356.0020.

Synthesis of BOAHY 2e

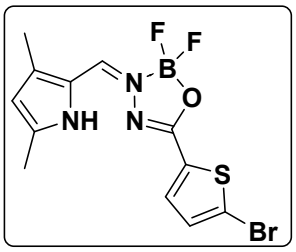

2e

To a round-bottom flask equipped with a magnetic stirring bar, 3,5-dimethyl-1H-pyrrole-2-carbaldehyde (123 mg, 1 mmol) and 5-bromothiophene-2-carbohydrazide (243 mg, 1.1 mmol) to afford the intermediate hydrazone, after simple concentration of the reaction mixture under vacuum, followed by addition of 10 mL dry toluene, triethylamine (0.5 mL) after which the reaction mixture was stirred for 10 minutes at 0 °C. $BF_3{\cdot}Et_2O$ (1.0 mL) was then added dropwise and the mixture refluxed under nitrogen for 3h to afford the desired product **2e**.

Yield: 45%; mp: 216 – 217 °C.

^{1}H NMR (400 MHz, $CDCl_3$) δ 10.62 (bs, 1H), 7.54 (d, *J* = 4.0 Hz, 1H), 7.46 (s, 1H), 7.11 (d, *J* = 4.0 Hz, 1H), 6.03 (d, *J* = 2.6 Hz, 1H), 2.44 (s, 3H), 2.26 (s, 3H); ^{13}C NMR (101 MHz, $CDCl_3$) δ 163.23, 142.53, 139.29, 134.44, 132.46, 131.56, 131.41, 121.94, 119.33, 114.04, 14.25, 11.48; ^{11}B NMR (128 MHz, $CDCl_3$) δ 4.23 (t, *J* = 16.6 Hz); ^{19}F NMR (377 MHz, $CDCl_3$) δ -149.11 (dd, *J* = 33.5, 13.0 Hz); ^{19}F NMR (377 MHz, $CDCl_3$) δ -149.12 (dd, *J* = 33.6, 13.2 Hz).

HRMS (ESI, $[M + H]^+$) for $C_{12}H_{12}BBrF_2N_3OS$ calcd 373.9940, found 373.9944.

General procedure for post-functionalized BOAHY 2f-2g

A mixture of bromide BOAHY **2d** (to prepare **2f**) or **2e** (to prepare **2g**) (0.4 mmol), 4-butylphenylacetylene (1.0 mmol, 2.5 eq), CuI (14 mg), and $Pd(PPh_3)_2Cl_2$ (22 mg) was dissolved in 8 mL dry THF. Then 0.5 mL DIPEA was added to this mixture which was kept at reflux overnight under argon atmosphere. The cooled reaction mixture was quenched with water and extracted with DCM. The organic layer was washed with water, dried over magnesium sulfate and concentrated under reduced pressure. The residue was then purified by column chromatography (silica gel) using petroleum ether and DCM as eluent to afford the corresponding BOAHY as pure solids. The compound was then further purified by recrystallization from DCM-pentane solvent mixture.

Synthesis of BOAHY 2f

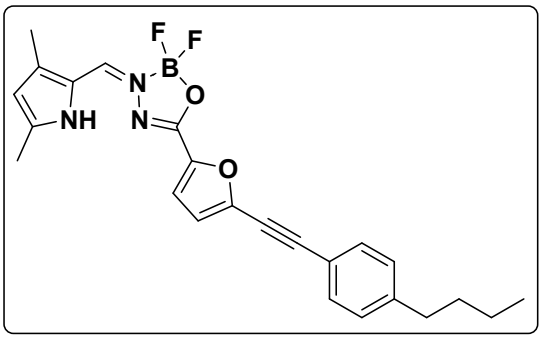

2f

Yield: 85%; mp: 181.5 – 182.5 °C.

^{1}H NMR (400 MHz, $CDCl_3$) δ 10.83 (bs, 1H), 7.53 (s, 1H), 7.48 (d, *J* = 8.2 Hz, 2H), 7.24 (d, *J* = 3.6 Hz, 1H), 7.20 (d, *J* = 8.2 Hz, 2H), 6.76 (d, *J* = 3.6 Hz, 1H), 6.04 (d, *J* = 2.3 Hz, 1H), 2.64 (t, *J* = 7.6 Hz, 2H), 2.46 (s, 3H), 2.30 (s, 3H), 1.69 – 1.56 (m, 2H), 1.37 (dq, *J* = 14.6, 7.4 Hz, 2H), 0.94 (t, *J* = 7.3 Hz, 3H); ^{13}C NMR (101 MHz, $CDCl_3$) δ 159.53, 144.98, 143.11, 142.87, 140.88, 139.33, 134.85, 131.78, 128.82, 122.05, 118.76, 118.52, 117.15, 114.12, 96.23, 78.45, 35.83, 33.43, 22.44, 14.36, 14.03, 11.50; ^{11}B NMR (128 MHz, $CDCl_3$) δ 4.19; ^{19}F NMR (376 MHz, $CDCl_3$) δ -149.36 (d, *J* = 25.4 Hz).

HRMS (ESI, $[M + H]^+$) for $C_{24}H_{24}BF_2N_3O_2$ calcd 436.2003, found 436.2003.

Synthesis of BOAHY 2g

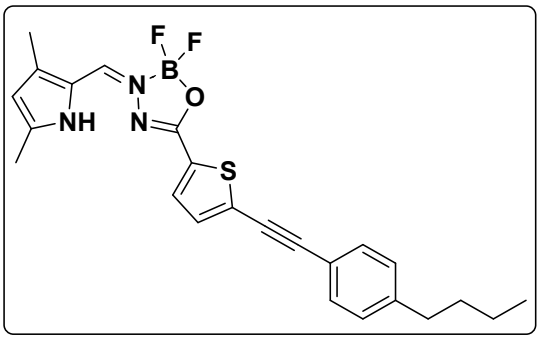

2g

Yield: 83%; mp: 222.5 – 223.5 °C.

^{1}H NMR (400 MHz, $CDCl_3$) δ 10.70 (bs, 1H), 7.70 (d, *J* = 3.9 Hz, 1H), 7.48 (s, 1H), 7.45 (d, *J* = 8.1 Hz, 2H), 7.24 (d, *J* = 3.9 Hz, 1H), 7.19 (d, *J* = 8.1 Hz, 2H), 6.04 (d, *J* = 2.6 Hz, 1H), 2.63 (t, *J* = 7.7 Hz, 2H), 2.45 (s, 3H), 2.28 (s, 3H), 1.67 – 1.57 (m, 2H), 1.41 – 1.32 (m, 2H), 0.93 (t, *J* = 7.3 Hz, 3H); ^{13}C NMR (101 MHz, $CDCl_3$) δ 163.52, 144.61, 142.41, 139.14, 134.28, 132.50, 132.20, 131.66, 130.35, 129.54, 128.78, 122.02, 119.38, 113.99, 96.98, 81.61, 35.81, 33.47,22.45, 14.28, 14.06, 11.50; ^{11}B NMR (128 MHz, $CDCl_3$) δ 4.31; ^{19}F NMR (376 MHz, $CDCl_3$) δ -149.15 (d, *J* = 30.3 Hz).

HRMS (ESI, $[M + H]^+$) for $C_{24}H_{24}BF_2N_3OS$ calcd 452.1774, found 452.1775.

2. Characterization Procedures

General Characterization Procedures

Chemicals received from commercial sources were used without further purification. Reaction dry solvents (toluene and THF) were dried using a M- Braun SPS-800 system. TLC were carried out on Kieselgel 60 F254 plates (Merck) and visualized with UV lamp 254/365 nm. For column chromatography 70-230 mesh silica 60 (E. M. Merck) was used as the stationary phase. NMR spectra were recorded on a Bruker Avance (400 MHz) or a Bruker Avance (600 MHz) spectrometer at room temperature, and chemical shifts (δ) are reported part per million (ppm) referenced to tetramethylsilane (TMS, 0.0 ppm), ($CDCl_3$, 7.26 ppm for ^1H NMR and 77.16 ppm for ^{13}C NMR), (DMSO, 2.50 ppm for ^1H NMR and 39.52 ppm for ^{13}C NMR). Melting points were determined using a Reichert Thermovar apparatus. High-resolution mass spectra (HRMS) were detected by a quadrupole orthogonal acceleration time-of-flight mass spectrometer (Synapt G2 HDMS, Waters, Milford, MA). Samples were infused at 3μL/min and spectra were obtained in positive ionization mode with a resolution of 15000 (FWHM) using leucine enkephalin as lock mass.

X-Ray Crystallography

Single crystals suitable for X-ray diffraction were obtained by slow evaporation of DCM solutions at room temperature. X-ray intensity data were collected at 293(2) K on an Agilent SuperNova diffractometer with Eos CCD detector using MoKα radiation (λ = 0.71073 Å). Data frames were processed (unit cell determination, intensity data integration, correction for Lorentz and polarization effects, and empirical absorption correction) using CrysAlis PRO[1]. The structures were solved using Olex2[2] with the ShelXT[3] structure solution program using Intrinsic Phasing and refined with the ShelXL[4] refinement package using full-matrix least-squares minimization on F2. CCDC 2276919, 2276920 and 2277472-2277476 contain the supplementary crystallographic data for this paper and can be obtained free of charge via http://www.ccdc.cam.ac.uk/getstructures or from the Cambridge Crystallographic Data Centre, 12, Union Road, Cambridge CB2 1EZ, UK; fax: +44-1223-336033; deposit@ccdc.cam.ac.uk).

Steady-State Spectroscopy

Dilute solutions were prepared by dissolving the dyes in heptane, acetonitrile, methyltetrahydrofuran and water/acetonitrile mixtures and sonicating for 5 minutes. All solvents were spectroscopic grade and used without further purification. Steady-state UV/VIS absorption spectra of the dye solutions were measured on a Perkin Elmer Lambda 950 spectrometer in quartz cuvettes (1 cm path length). Diffuse reflectance spectra of the solid state

dyes in quartz cuvettes (1 mm path length) were acquired using the same spectrometer and converted into Kubelka-Munk equivalent absorbance. A Horiba Jobin Yvon Fluorolog 3 spectrofluorometer in right-angle configuration was used to record the emission spectra of the solutions and the solid state dyes. Low-temperature (77K) emission and excitation spectra were measured on a Edinburgh FLS980 spectrofluorometer. Quantum yields were determined with the integrating sphere technique employing the aforementioned Horiba spectrofluorometer. A 420 nm longpass filter was used on the detector side to avoid second-order scattering effects when collecting the fluorescence spectra. Using a quantum counter, the excitation spectra were corrected for the wavelength dependence of the intensity of the excitation light as well as for temporal fluctuations of this intensity. The emission spectra were corrected for the wavelength dependence of the detection channel throughput. All steady-state spectra were processed using Origin software.

Time-Correlated Single Photon Counting

Fluorescence decay times at the picosecond-nanosecond time scale were determined by time-correlated single photon counting (TCSPC). The output of a mode-locked Ti:sapphire laser (Tsunami, Spectra Physics) was used as the excitation light. The linearly polarized excitation light was rotated to a vertical direction by the use of a Berek compensator (New Focus) in combination with a polarization filter and directed onto the sample. The solution was placed in a quartz cuvette (1 cm path length) and sealed by a Teflon stopper and then mounted on the device. The emission was collected under 90° with respect to the incident light and guided through a polarization filter that was set at the magic angle (54.7°) with respect to the polarization of the excitation beam. The fluorescence was spectrally resolved by a monochromator (Sciencetech 9030, 100 nm focal length, wavelength accuracy 0.3 nm) and detected by a microchannel plate photomultiplier tube (MCP-PMT, R3809U-51, Hamamatsu). A time-correlated single-photon timing PC module (SPC 830, Becker & Hickl) was used to obtain the fluorescence decay histogram in 4096 channels. The decays were recorded with 10 000 counts in the peak channel, in time windows of 16 ns, and analyzed individually with a time-resolved fluorescence analysis (TRFA) software. The full width at half-maximum (FWHM) of the IRF was typically in the order of 42 ps. By fitting the experimental data to a convolution of a multi-exponential decay with the instrument response function (IRF) via a non-linear least square method, the fluorescence lifetimes and corresponding amplitudes were calculated. The quality of the fit was monitored by the value of χ^2 (<1.3) and by visual inspection of the residuals and their autocorrelation function.

Femtosecond Fluorescence Up-Conversion

Fluorescence decay times at the femtosecond-picosecond time scale were determined by femtosecond fluorescence up-conversion. An amplified femtosecond double OPA laser system was used to generate the excitation and gate pulses. The assembly of a Ti:sapphire oscillator (Mai Tai SP, Spectra-Physics) coupled to a laser amplifier comprising a stretcher, Ti:sapphire regenerative cavity amplifier and compressor (Spitfire Pro 35F-XP, Spectra-Physics) is the source of 35-fs pulses (FWHM), 31-nm bandwidth (FWHM), 4 mJ in the 800-nm range and has a repetition rate of 1 kHz. The regenerative amplifier is energized by a Q-switched, diode-pumped Nd:YLF pulsed laser (Empower-30, Spectra-Physics) capable of delivering 527 nm output beam of 30 Watts. The output of the amplifier is used to pump two identical two-stage optical parametric amplifiers (OPA) of white-light continuum (Topas-C, Light Conversion). Each (OPA) is pumped with 1 mJ pulse energy producing 60 fs (FWHM), 31 nm bandwidth (FWHM), independently tunable excitation pulses of about 100 μJ at 500 nm and the output can be tuned over a range between 300 and 2600 nm. Less than 1 percent of the 800 nm amplifier output is used as gate pulses and routed towards the crystal via a computer controlled translation stage to obtain a relative delay between excitation and gate pulses. The power of the excitation beam was set to 150 μW. The fluorescence light emitted from the sample (in an 1 mm quartz cuvette) was efficiently collected using an off-axis parabolic mirror, filtered to suppress the scattered light, directed and overlapped with a gate pulse (800 nm, ca. 10 μJ) derived from the regenerative amplifier in an BBO crystal (thickness 1 mm). By tuning the incident angle of these two beams relative to the crystal plane the sum frequency of the fluorescence light and the gate pulse was generated. A photomultiplier tube (R1527, Hamamatsu), placed at the exit of a 30 cm monochromator was used (heterodyne mode). The fluorescence decays traces are then recorded by detecting this sum frequency light while changing the relative delay of the gate pulse versus the sample excitation pulse. The prompt response of this arrangement (including laser sources) was determined by cross-correlation between pump and gate pulses and found to be less than 100 fs (FWHM).

3. X-Ray Crystallography

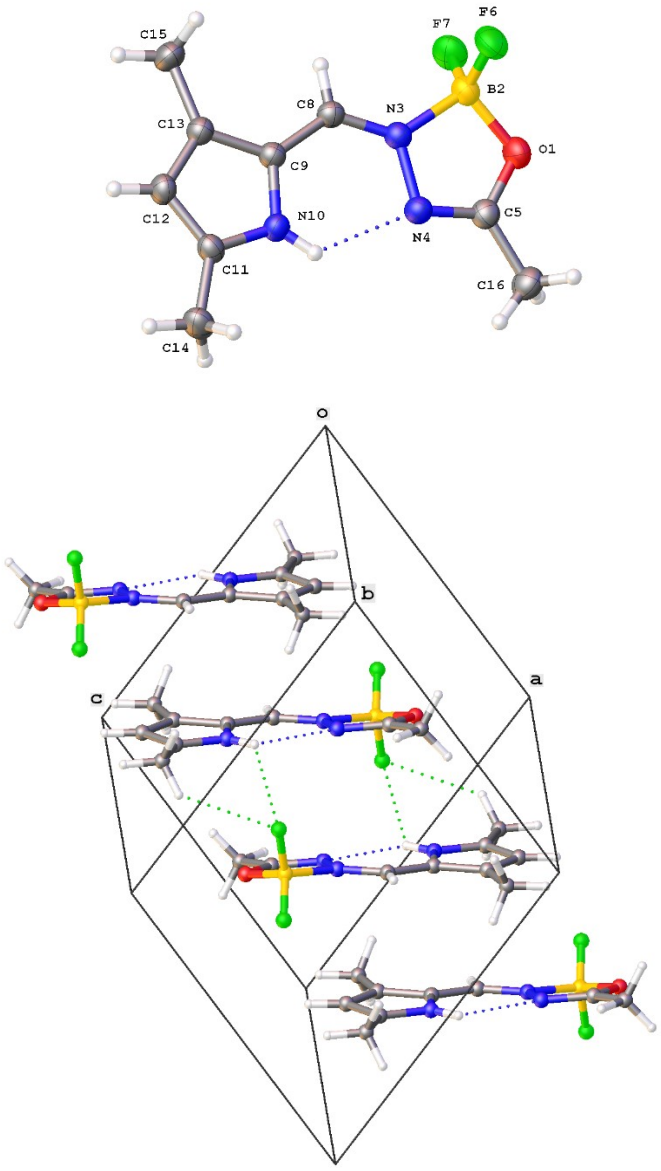

Fig. S1. Molecular structure of **2a**, with atom labels and thermal displacement ellipsoids drawn at the 30% probability level, and crystal packing, obtained from X-ray crystallography.

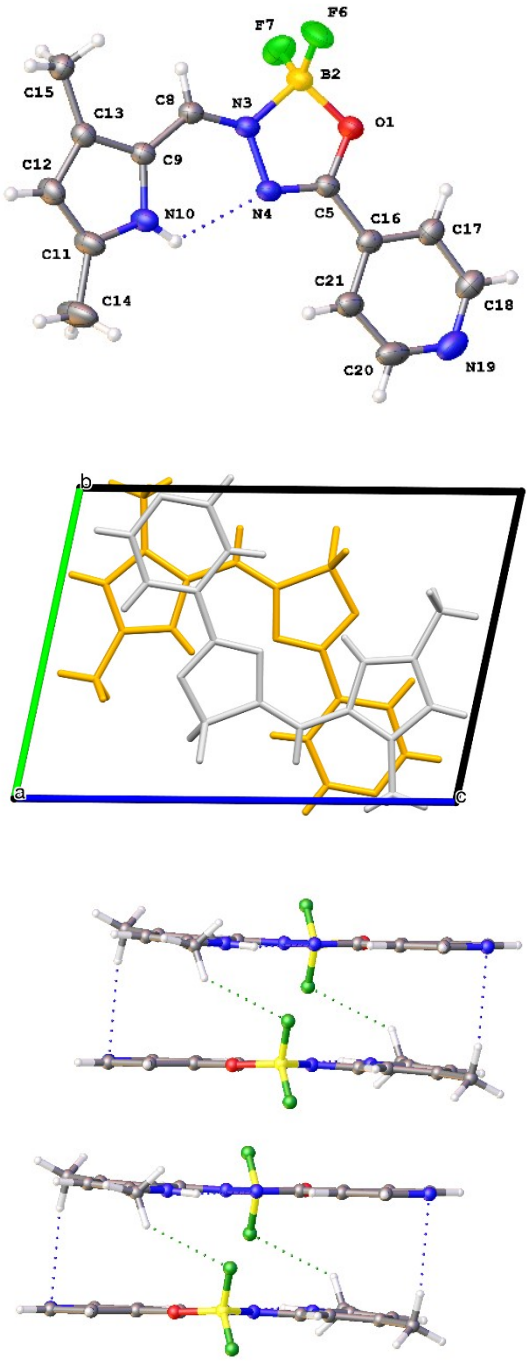

Fig. S2. Molecular structure of **2b**, with atom labels and thermal displacement ellipsoids drawn at the 30% probability level, and crystal packing, obtained from X-ray crystallography.

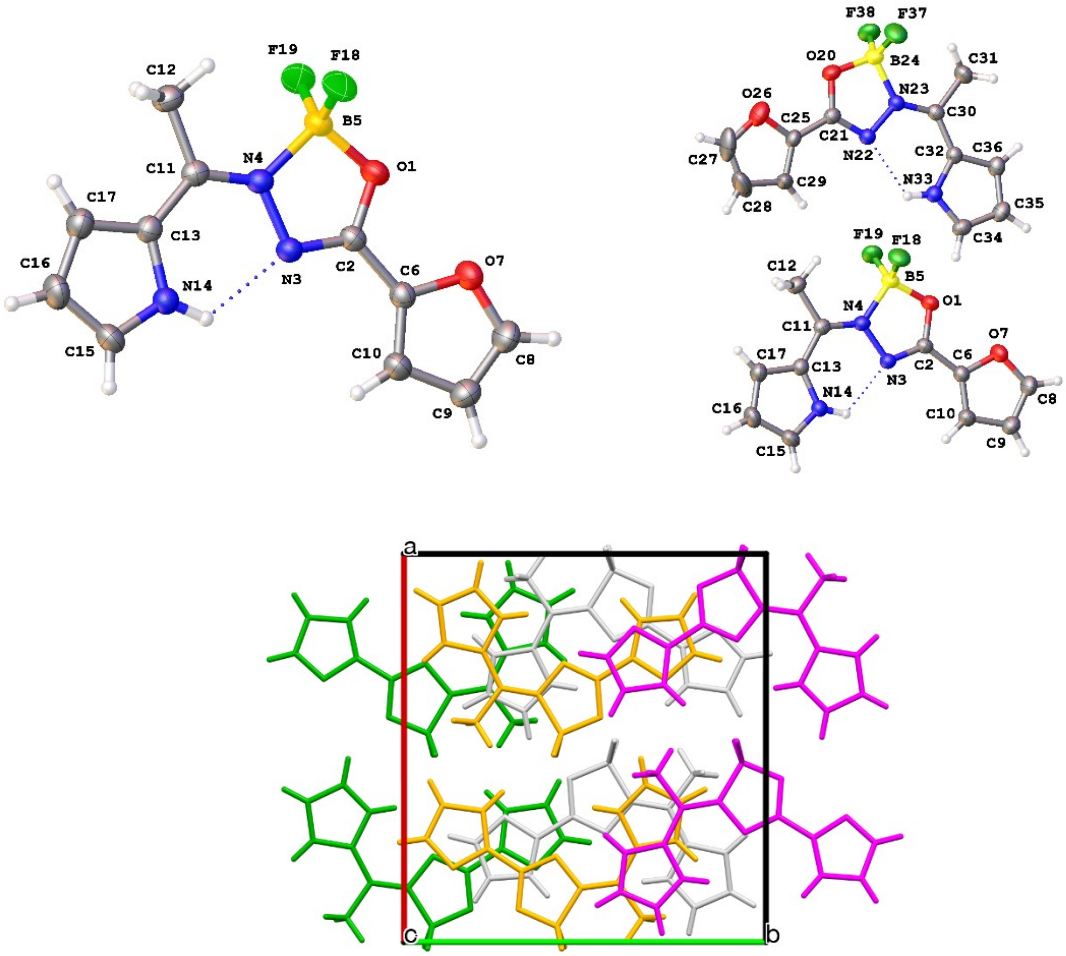

Fig. S3. Molecular structure of **2c**, with atom labels and thermal displacement ellipsoids drawn at the 30% probability level, and crystal packing, obtained from X-ray crystallography.

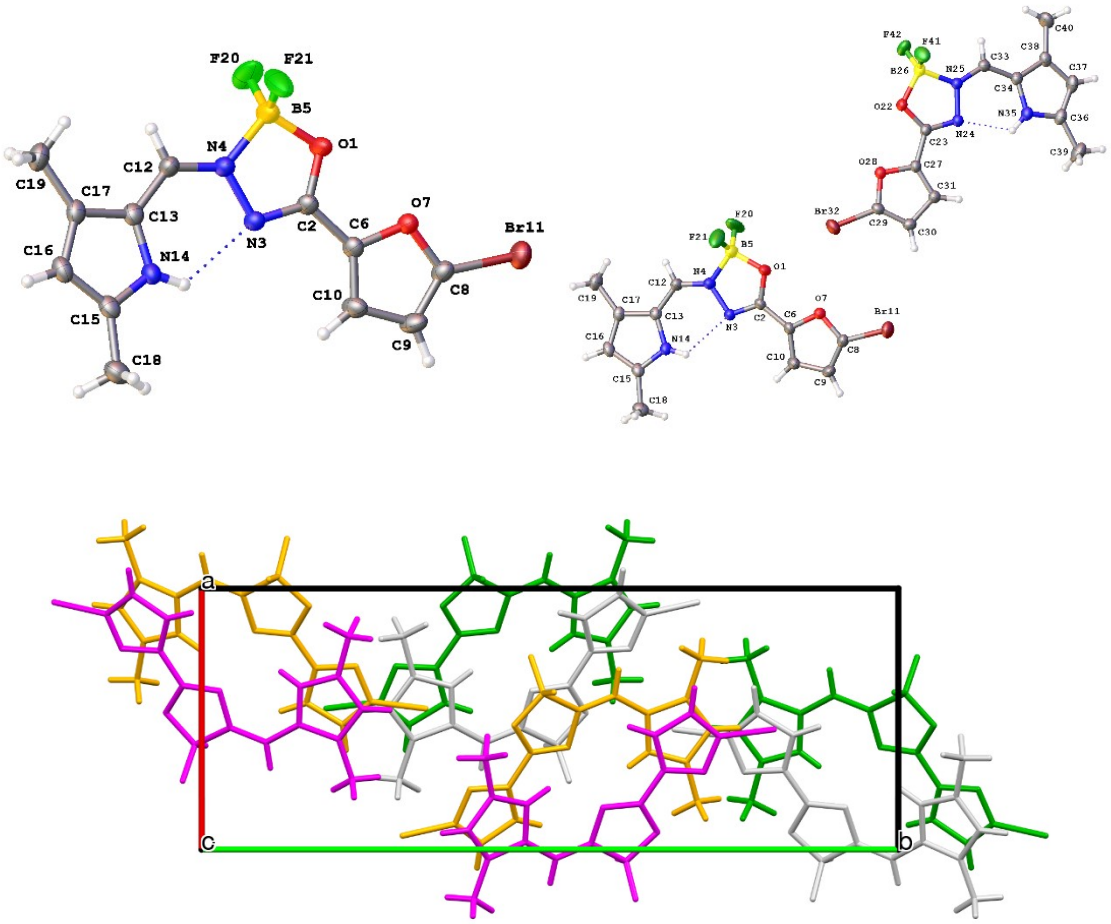

Fig. S4. Molecular structure of **2d**, with atom labels and thermal displacement ellipsoids drawn at the 30% probability level, and crystal packing, obtained from X-ray crystallography

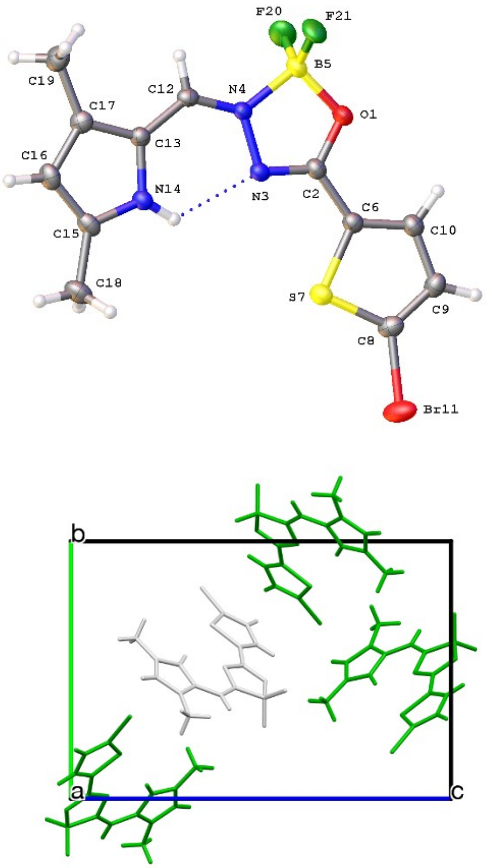

Fig. S5. Molecular structure of **2e**, with atom labels and thermal displacement ellipsoids drawn at the 30% probability level, and crystal packing, obtained from X-ray crystallography

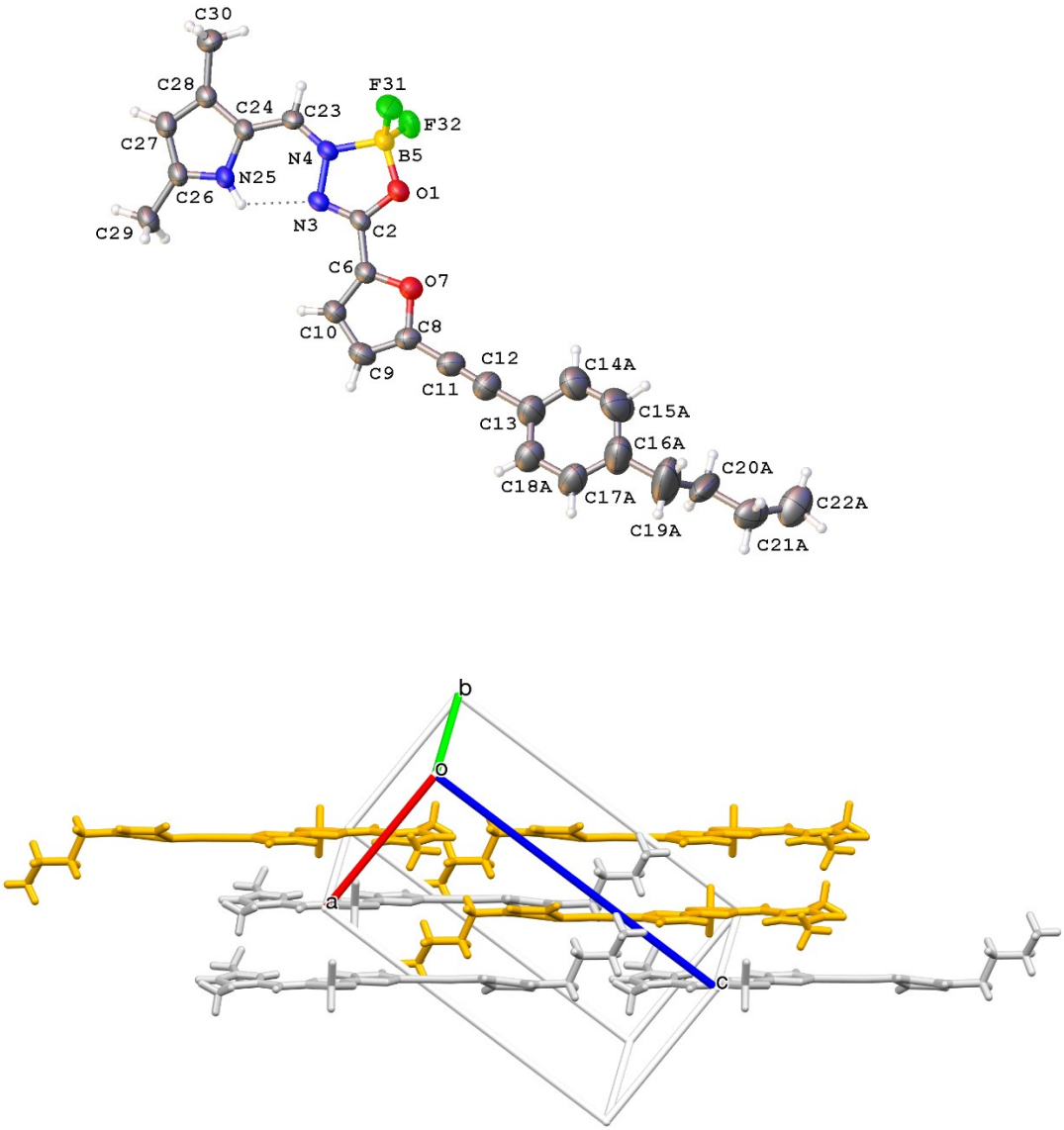

Fig. S6. Molecular structure of **2f**, with atom labels and thermal displacement ellipsoids drawn at the 30% probability level, and crystal packing, obtained from X-ray crystallography. For clarity only one part of the disordered region is shown.

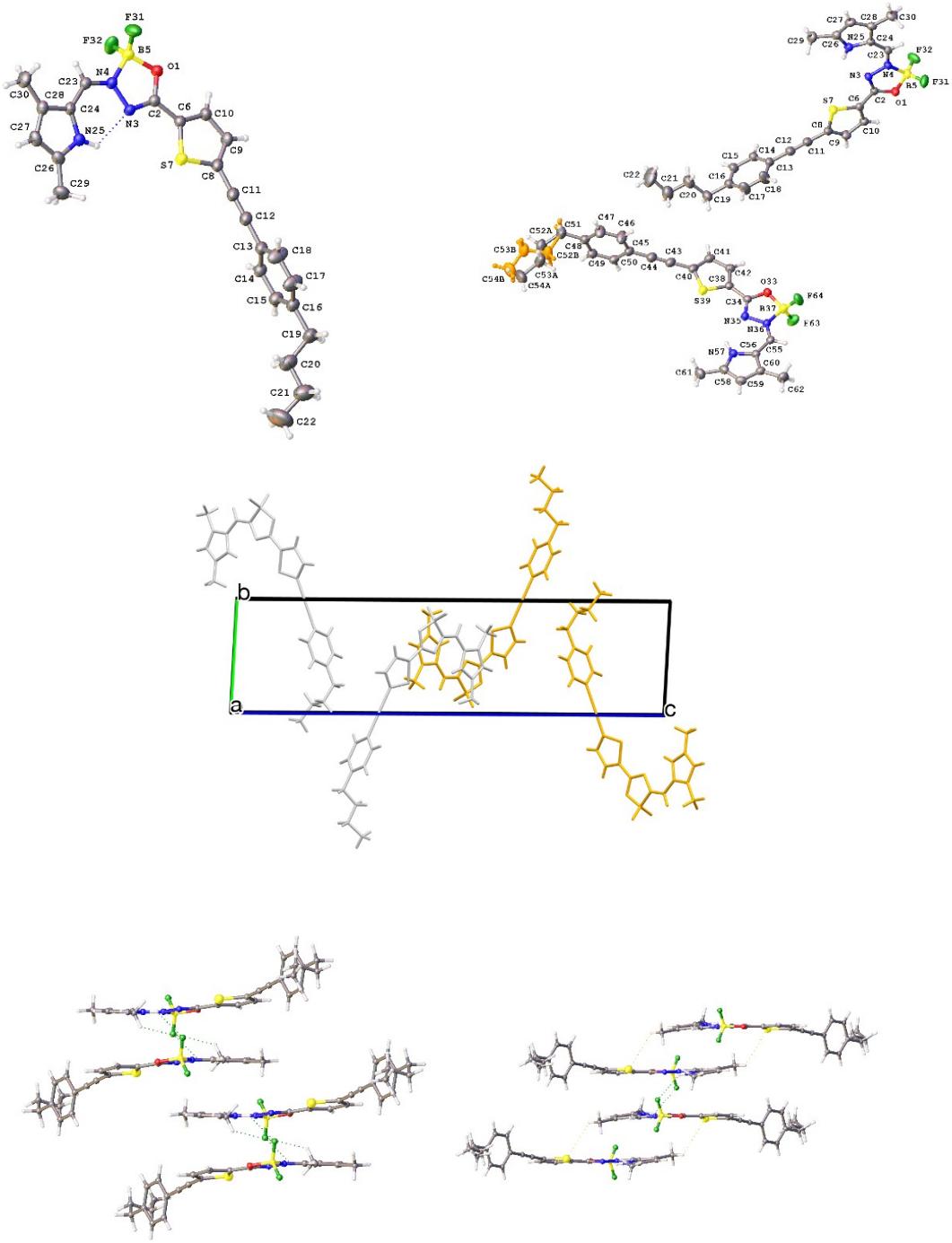

Fig. S7. Molecular structure of **2g**, with atom labels and thermal displacement ellipsoids drawn at the 30% probability level, and crystal packing, obtained from X-ray crystallography.

Table S1. Crystal data and structure refinement parameters for **2a** obtained from X-ray crystallography.

Parameter	2a
Empirical formula	$C_9H_{12}BF_2N_3O$
Formula weight	227.03
Temperature/K	293(2)
Crystal system	triclinic
Space group	P-1
a/Å	8.4328(6)
b/Å	8.6941(6)
c/Å	9.1341(6)
α/°	69.030(6)
β/°	74.586(6)
γ/°	63.527(7)
Volume/Å^3	555.21(8)
Z	2
ρ_{calc} g/cm^3	1.358
μ/mm^{-1}	0.112
F(000)	236.0
Crystal size/mm^3	0.5 × 0.3 × 0.3
Radiation	Mo Kα (λ = 0.71073)
2Θ range for data collection/°	4.814 to 52.74
Index ranges	$-10 \leq h \leq 10$, $-10 \leq k \leq 10$, $-11 \leq l \leq 11$
Reflections collected	11486
Independent reflections	2274 [R_{int} = 0.0314, R_{sigma} = 0.0265]
Data/restraints/parameters	2274/0/152
Goodness-of-fit on F2	1.031
Final R indexes [I>=2σ (I)]	R_1 = 0.0506, wR_2 = 0.1254
Final R indexes [all data]	R_1 = 0.0715, wR_2 = 0.1411
Largest diff. peak/hole / e Å^{-3}	0.21/-0.25

Table S2. Crystal data and structure refinement parameters for **2b**-**2c** obtained from X-ray crystallography.

Parameter	2b	2c
Empirical formula	$C_{13}H_{13}BF_2N_4O$	$C_{22}H_{20}B_2F_4N_6O_4$
Formula weight	290.08	530.06
Temperature/K	293(2)	294(2)
Crystal system	triclinic	monoclinic
Space group	P-1	P21/c
a/Å	7.0441(5)	14.3453(6)
b/Å	8.8128(5)	12.6030(6)
c/Å	12.0934(7)	14.0398(8)
α/°	76.688(5)	90
β/°	80.661(6)	109.496(5)
γ/°	76.058(6)	90
Volume/Å^3	704.50(8)	2392.8(2)
Z	2	4
ρ_{calc} g/cm^3	1.367	1.471
μ/mm^{-1}	0.107	0.122
F(000)	300.0	1088.0
Crystal size/mm^3	0.3 × 0.25 × 0.25	0.4 × 0.35 × 0.2
Radiation	MoKα (λ = 0.71073)	Mo Kα (λ = 0.71073)
2Θ range for data collection/°	4.86 to 52.742	4.776 to 52.744
Index ranges	-8 ≤ h ≤ 8, -11 ≤ k ≤ 11, -15 ≤ l ≤ 15	-17 ≤ h ≤ 17, -15 ≤ k ≤ 15, -17 ≤ l ≤ 17
Reflections collected	14570	24766
Independent reflections	2876 [Rint = 0.0220, Rsigma = 0.0185]	4885 [Rint = 0.0393, Rsigma = 0.0347]
Data/restraints/parameters	2876/0/196	4885/0/346
Goodness-of-fit on F2	1.077	1.036
Final R indexes [I>=2σ (I)]	R1 = 0.0474, wR2 = 0.1283	R1 = 0.0533, wR2 = 0.1351
Final R indexes [all data]	R1 = 0.0641, wR2 = 0.1403	R1 = 0.0851, wR2 = 0.1597
Largest diff. peak/hole / e Å^{-3}	0.24/-0.21	0.33/-0.23

Table S3. Crystal data and structure refinement parameters for **2d** and **2e** obtained from X-ray crystallography.

Parameter	2d	2e
Empirical formula	$C_{24}H_{22}B_2Br_2F_4N_6O_4$	$C_{12}H_{11}BBrF_2N_3OS$
Formula weight	715.91	374.02
Temperature/K	293(2)	293(2)
Crystal system	monoclinic	orthorhombic
Space group	$P2_1/c$	P212121
a/Å	8.9571(6)	6.5546(4)
b/Å	23.2895(12)	12.4015(9)
c/Å	13.9900(9)	18.2966(10)
α/°	90	90
β/°	103.199(7)	90
γ/°	90	90
Volume/Å^3	2841.3(3)	1487.27(16)
Z	4	4
ρ_{calc} g/cm^3	1.674	1.670
μ/mm^{-1}	2.922	2.926
F(000)	1424.0	744.0
Crystal size/mm^3	0.35 × 0.15 × 0.15	0.55 × 0.3 × 0.3
Radiation	Mo Kα (λ = 0.71073)	Mo Kα (λ = 0.71073)
2Θ range for data collection/°	4.988 to 52.744	5.534 to 52.716
Index ranges	$-10 \le h \le 11$, $-29 \le k \le 29$, $-17 \le l \le 17$	$-8 \le h \le 6$, $-15 \le k \le 14$, $-22 \le l \le 22$
Reflections collected	29616	8962
Independent reflections	5805 [R_{int} = 0.0445, R_{sigma} = 0.0417]	3039 [R_{int} = 0.0265, R_{sigma} = 0.0362]
Data/restraints/parameters	5805/0/391	3039/0/196
Goodness-of-fit on F2	1.007	1.056
Final R indexes [I>=2σ (I)]	R_1 = 0.0454, wR_2 = 0.0873	R_1 = 0.0347, wR_2 = 0.0661
Final R indexes [all data]	R_1 = 0.0833, wR_2 = 0.1013	R_1 = 0.0497, wR_2 = 0.0715
Largest diff. peak/hole / e Å^{-3}	0.41/-0.45	0.24/-0.52

Table S4. Crystal data and structure refinement parameters for **2f** and **2g** obtained from X-ray crystallography.

Parameter	2f	2g
Empirical formula	$C_{24}H_{24}BF_2N_3O_2$	$C_{24}H_{24}BF_2N_3OS$
Formula weight	435.27	451.33
Temperature/K	293(2)	293(2)
Crystal system	triclinic	triclinic
Space group	P-1	P-1
a/Å	8.5264(4)	8.6651(3)
b/Å	8.9825(5)	9.2403(3)
c/Å	17.3830(13)	32.1446(10)
α/°	100.344(5)	86.941(2)
β/°	92.262(5)	89.022(3)
γ/°	113.518(5)	65.310(3)
Volume/Å^3	1191.76(13)	2335.10(14)
Z	2	4
ρ_{calc} g/cm^3	1.213	1.284
μ/mm^{-1}	0.088	0.175
F(000)	456.0	944.0
Crystal size/mm^3	0.4 × 0.3 × 0.05	0.55 × 0.1 × 0.1
Radiation	Mo Kα (λ = 0.71073)	Mo Kα (λ = 0.71073)
2Θ range for data collection/°	5.062 to 52.736	4.958 to 52.744
Index ranges	-10 ≤ h ≤ 10, -11 ≤ k ≤ 11, -21 ≤ l ≤ 21	-10 ≤ h ≤ 10, -11 ≤ k ≤ 11, -40 ≤ l ≤ 40
Reflections collected	19076	47736
Independent reflections	4863 [R_{int} = 0.0558, R_{sigma} = 0.0795]	9539 [R_{int} = 0.0427, R_{sigma} = 0.0414]
Data/restraints/parameters	4863/162/374	9539/6/620
Goodness-of-fit on F2	1.036	1.037
Final R indexes [I>=2σ (I)]	R_1 = 0.0966, wR_2 = 0.2568	R_1 = 0.0649, wR_2 = 0.1338
Final R indexes [all data]	R_1 = 0.1977, wR_2 = 0.3255	R_1 = 0.1018, wR_2 = 0.1527
Largest diff. peak/hole / e Å^{-3}	0.25/-0.18	0.30/-0.25

4. Steady-State Spectroscopy

4.1. Photophysical Properties

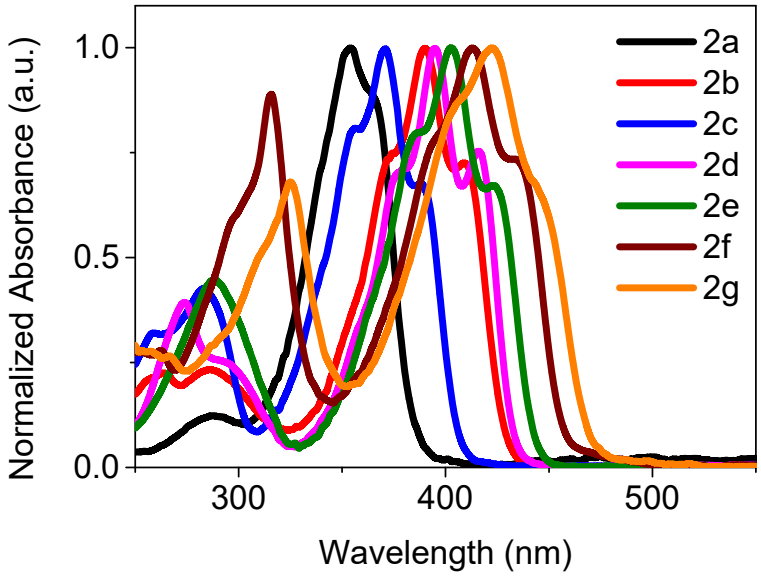

Fig. S8. Normalized absorption spectra of **2a**-**2g** in acetonitrile.

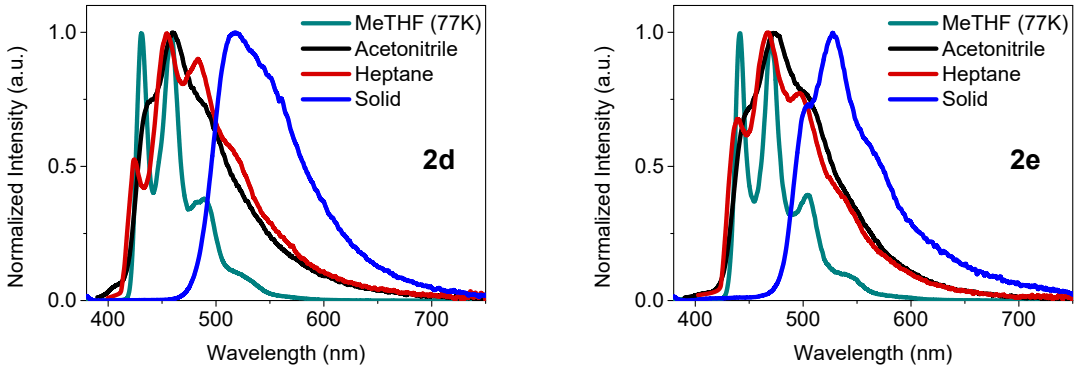

Fig. S9. Normalized emission spectra of **2d** and **2e** in different solvents and in solid state, excited at 360 nm.

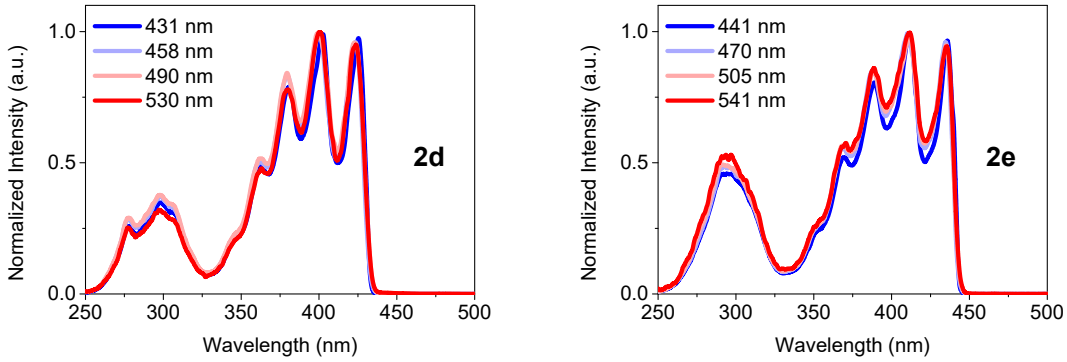

Fig. S10. Normalized excitation spectra of **2d** and **2e** in 2-methyltetrahydrofuran (MeTHF) at 77K, at different detection wavelengths.

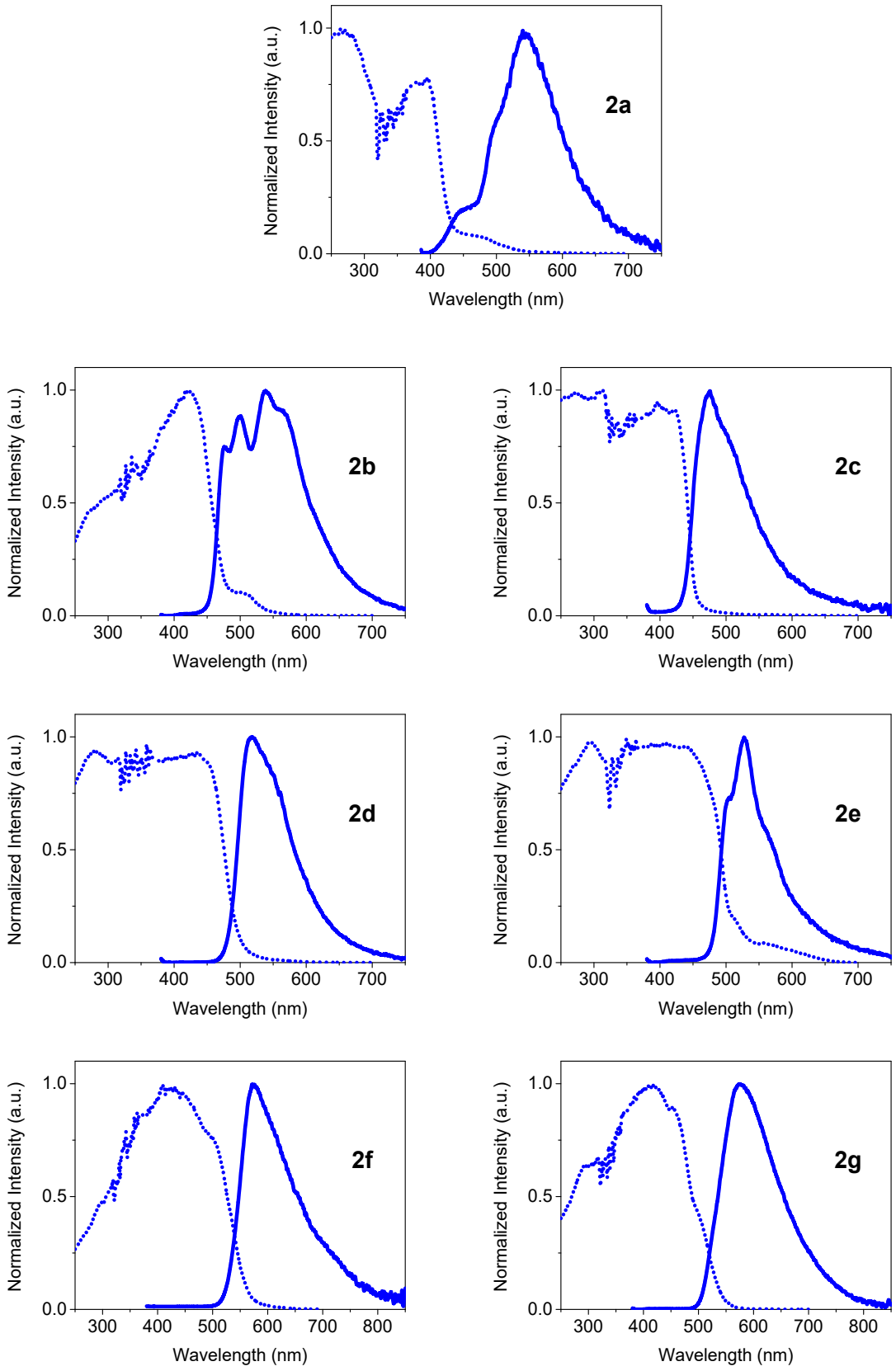

Fig. S11. Normalized absorption (Kubelka-Munk function) and emission spectra of **2a**-**2g** in solid state, excited at 360 nm.

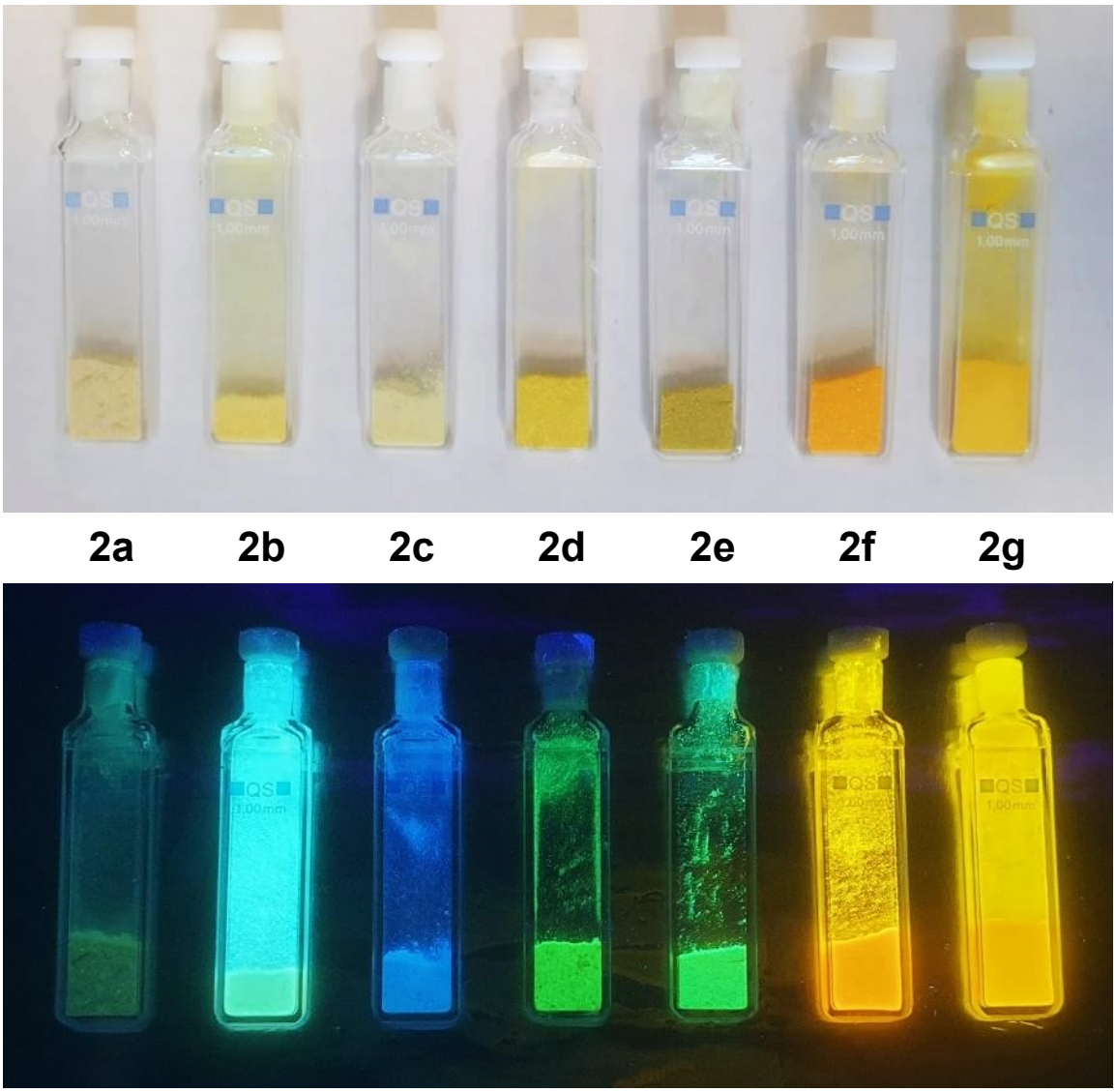

Fig. S12. Photograph of solid state **2a**-**2g** in daylight (top) and under 366 nm UV irradiation (bottom).

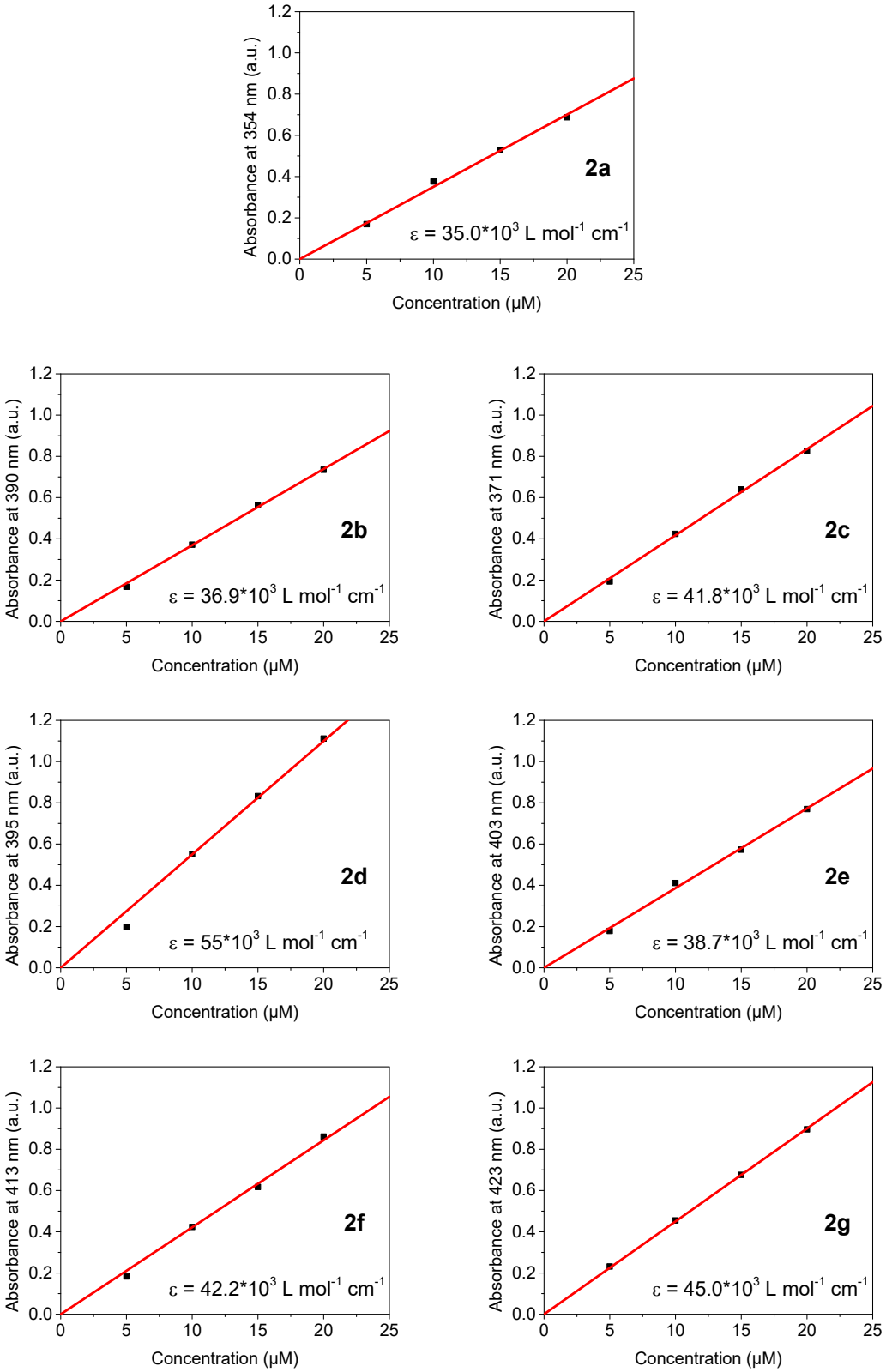

Fig. S13. Calibration curves and calculated molar extinction coefficients of **2a**-**2g** in acetonitrile.

4.2. Aggregation in Water/Acetonitrile Mixtures

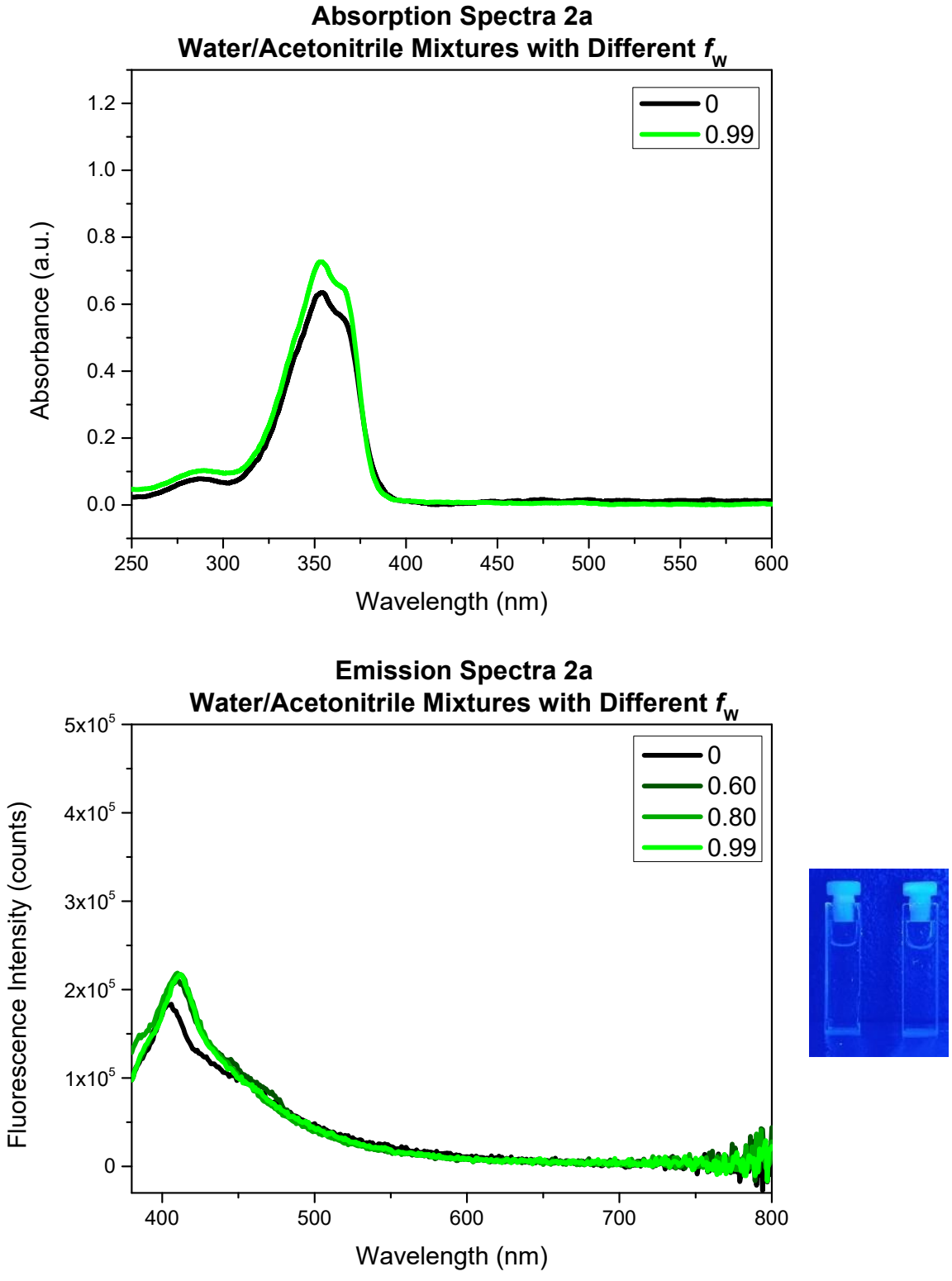

Fig. S14. Absorption (top) and emission (bottom) spectra of **2a** (2.0×10^{-5} mol/L) in water/acetonitrile with different water fractions f_w, excited at 360 nm. Alongside: photograph of the solutions with $f_w = 0$ (left) and $f_w = 0.99$ (right) under 366 nm UV irradiation.

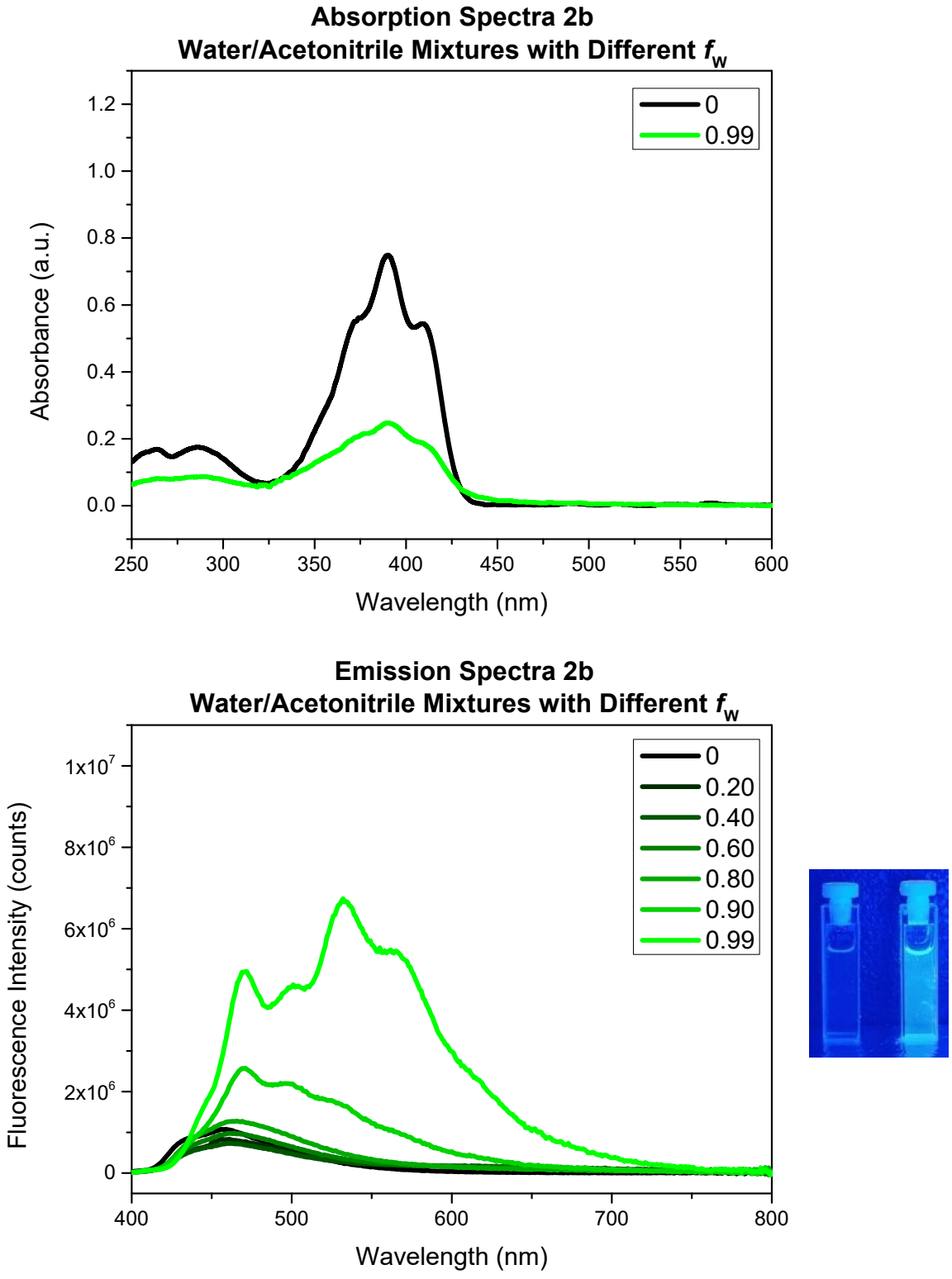

Fig. S15. Absorption (top) and emission (bottom) spectra of **2b** (2.0×10^{-5} mol/L) in water/acetonitrile with different water fractions f_w, excited at 360 nm. Alongside: photograph of the solutions with $f_w = 0$ (left) and $f_w = 0.99$ (right) under 366 nm UV irradiation.

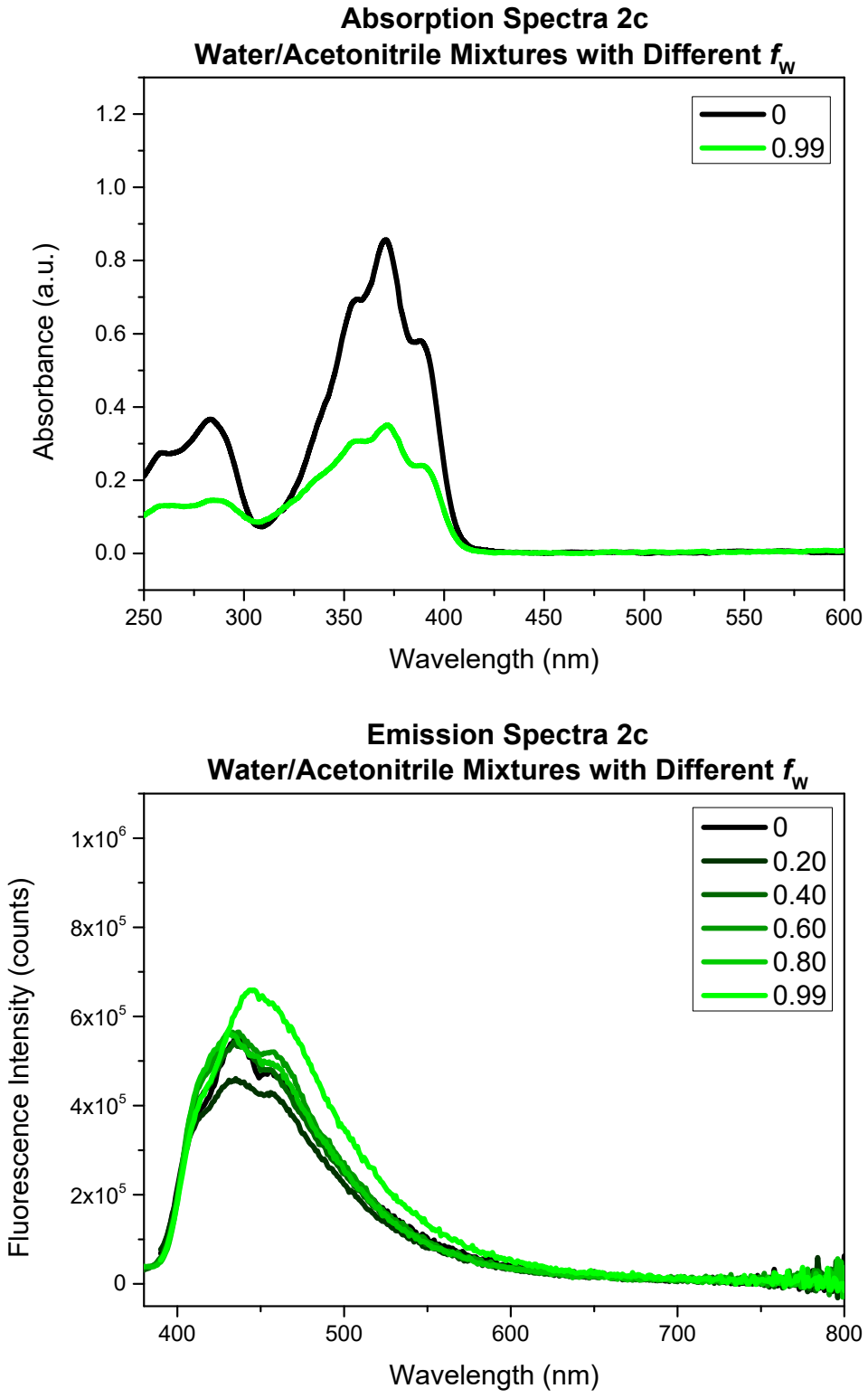

Fig. S16. Absorption (top) and emission (bottom) spectra of **2c** (2.0×10^{-5} mol/L) in water/acetonitrile with different water fractions f_w, excited at 360 nm. Alongside: photograph of the solutions with $f_w = 0$ (left) and $f_w = 0.99$ (right) under 366 nm UV irradiation.

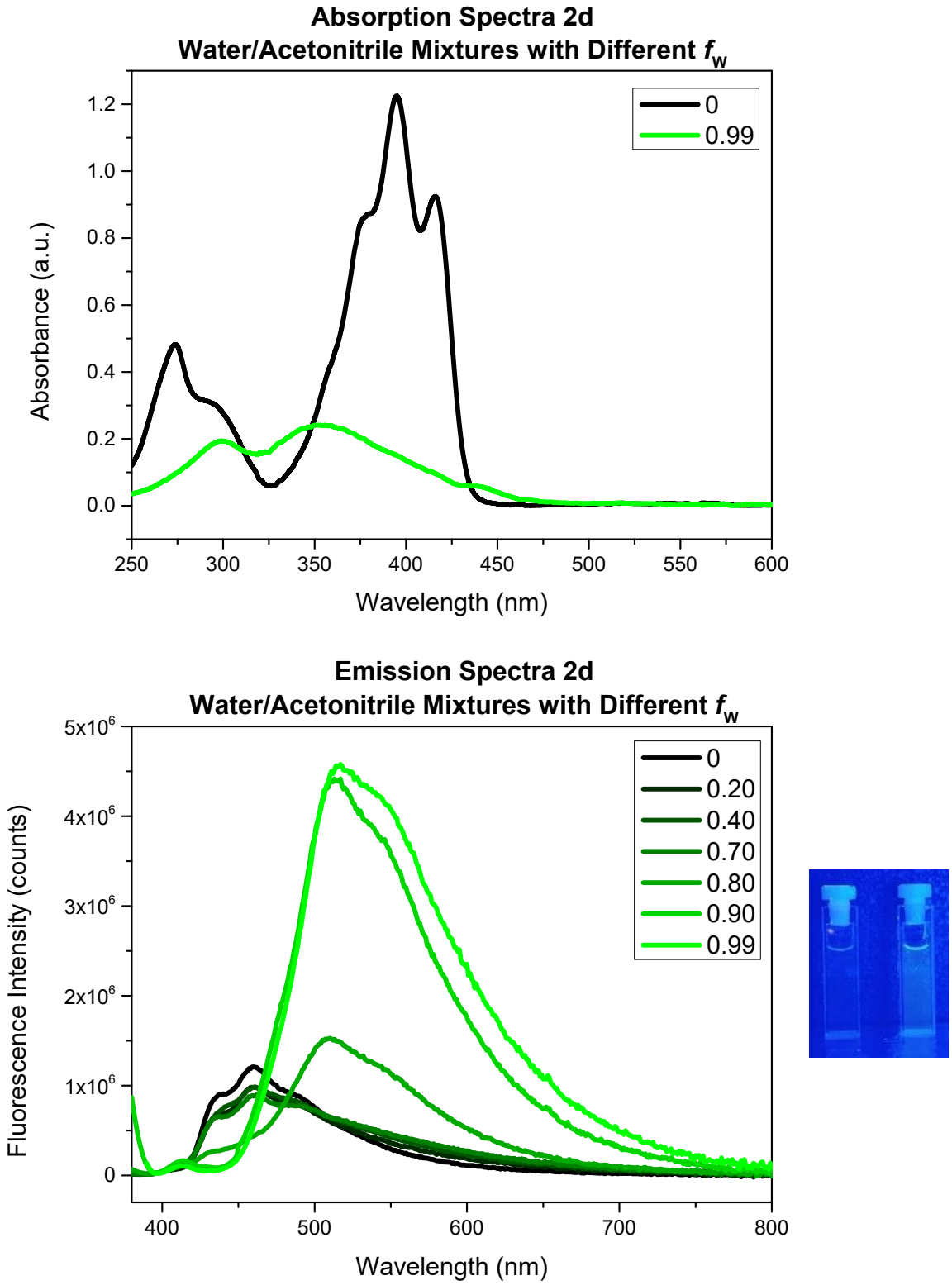

Fig. S17. Absorption (top) and emission (bottom) spectra of **2d** (2.0×10^{-5} mol/L) in water/acetonitrile with different water fractions f_w, excited at 360 nm. Alongside: photograph of the solutions with $f_w = 0$ (left) and $f_w = 0.99$ (right) under 366 nm UV irradiation.

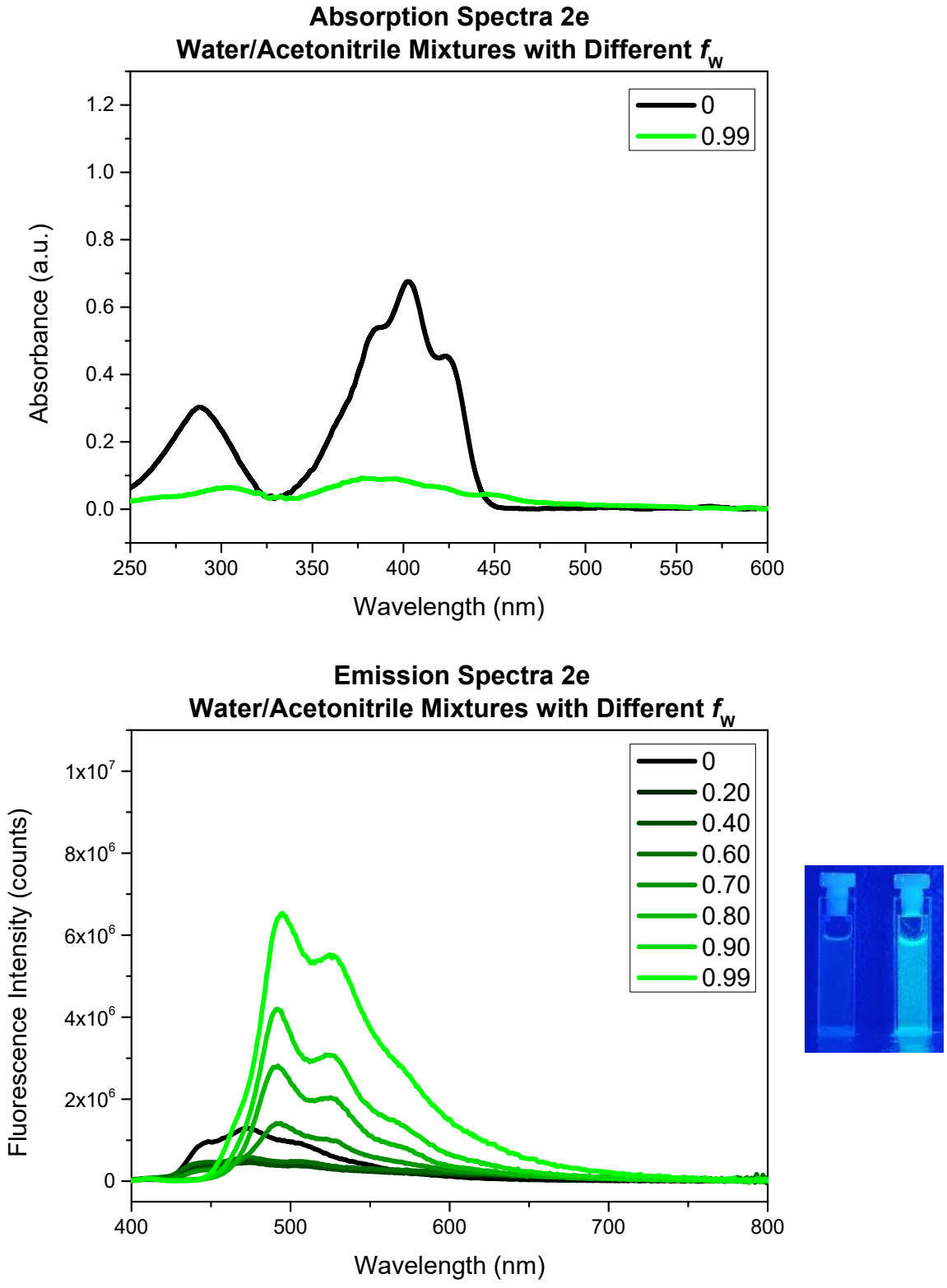

Fig. S18. Absorption (top) and emission (bottom) spectra of **2e** (2.0×10^{-5} mol/L) in water/acetonitrile with different water fractions f_w, excited at 360 nm. Alongside: photograph of the solutions with $f_w = 0$ (left) and $f_w = 0.99$ (right) under 366 nm UV irradiation.

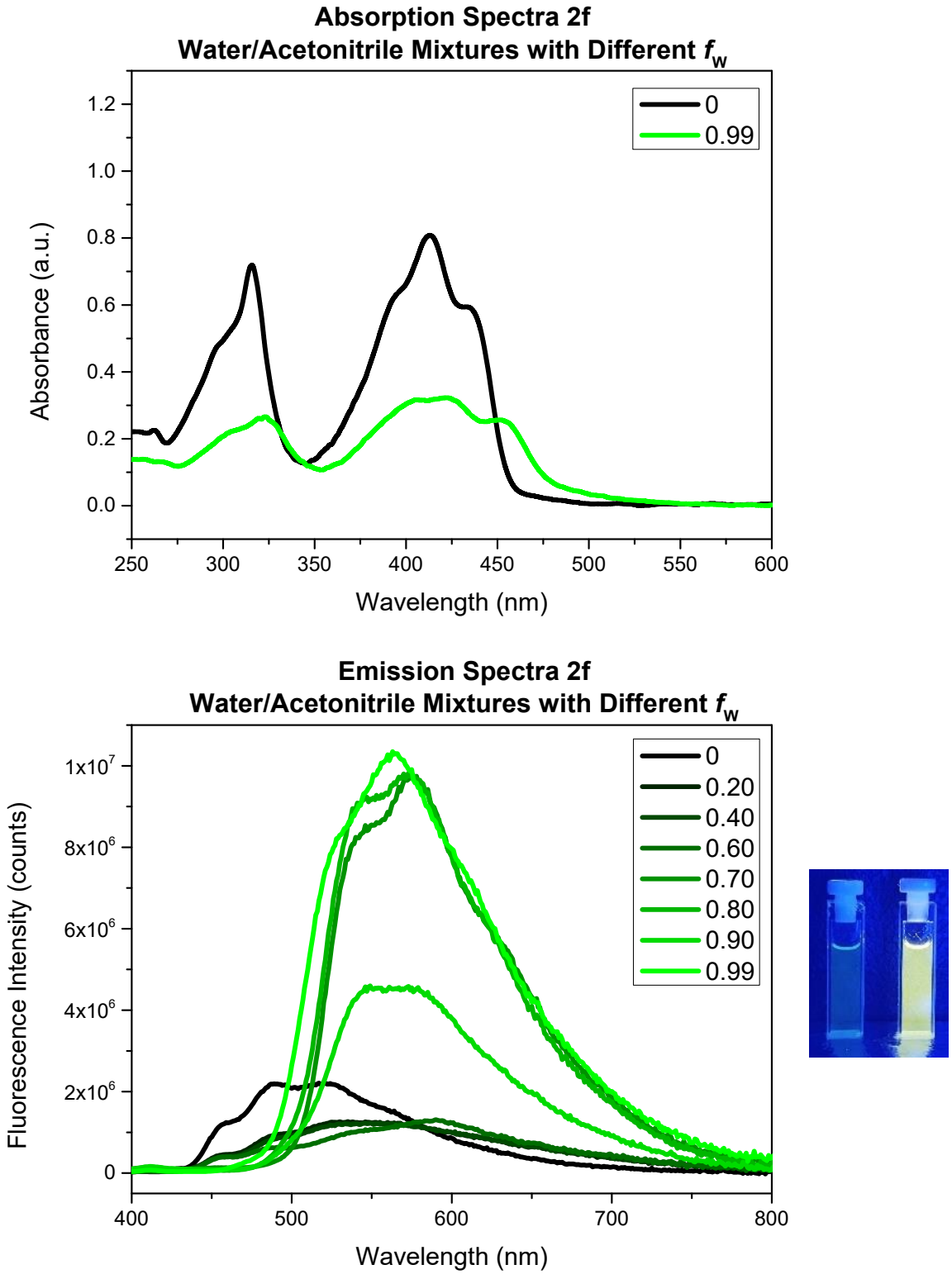

Fig. S19. Absorption (top) and emission (bottom) spectra of **2f** (2.0×10^{-5} mol/L) in water/acetonitrile with different water fractions f_w, excited at 360 nm. Alongside: photograph of the solutions with $f_w = 0$ (left) and $f_w = 0.99$ (right) under 366 nm UV irradiation.

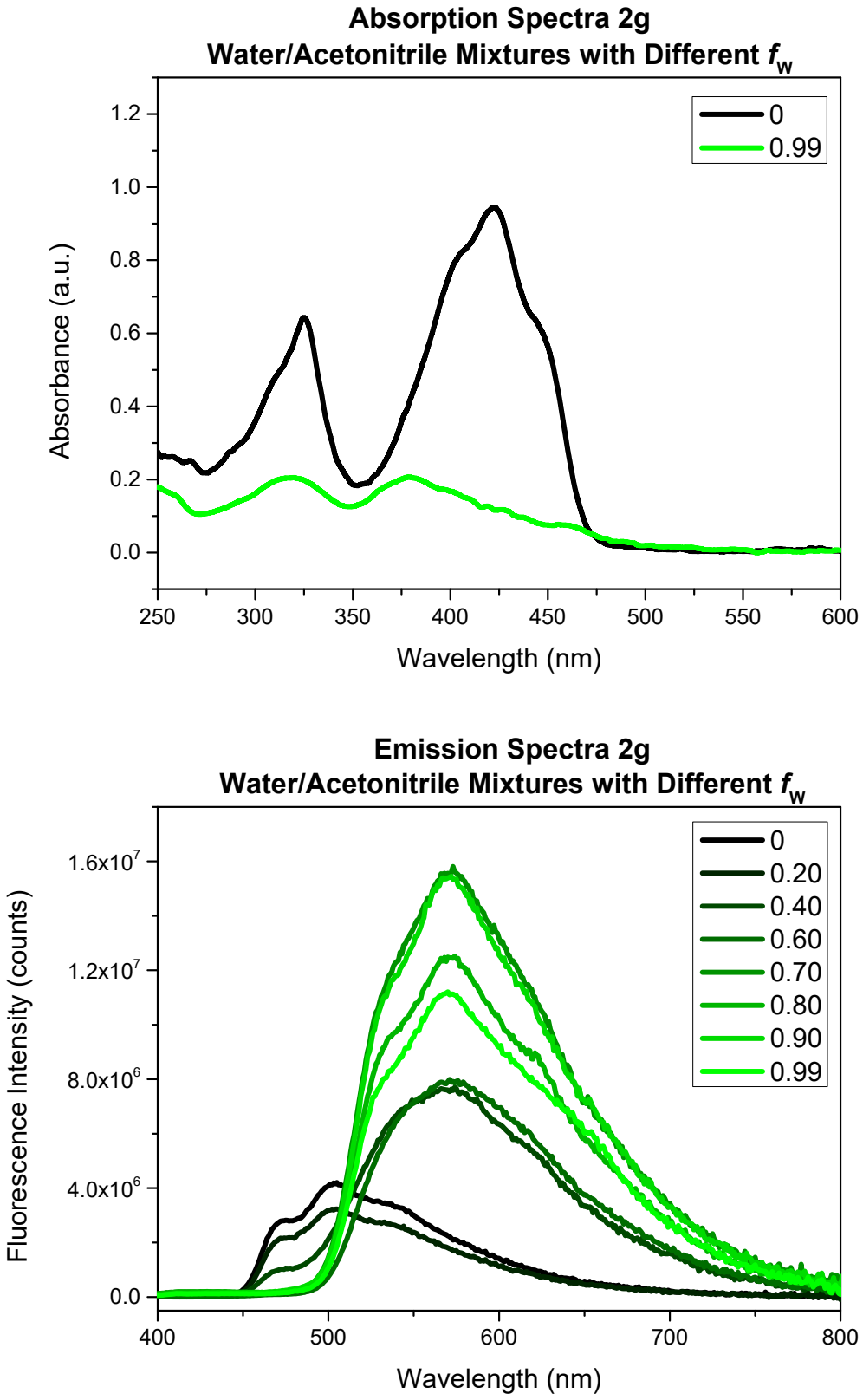

Fig. S20. Absorption (top) and emission (bottom) spectra of **2g** (2.0×10^{-5} mol/L) in water/acetonitrile with different water fractions f_w, excited at 360 nm. Alongside: photograph of the solutions with $f_w = 0$ (left) and $f_w = 0.99$ (right) under 366 nm UV irradiation.

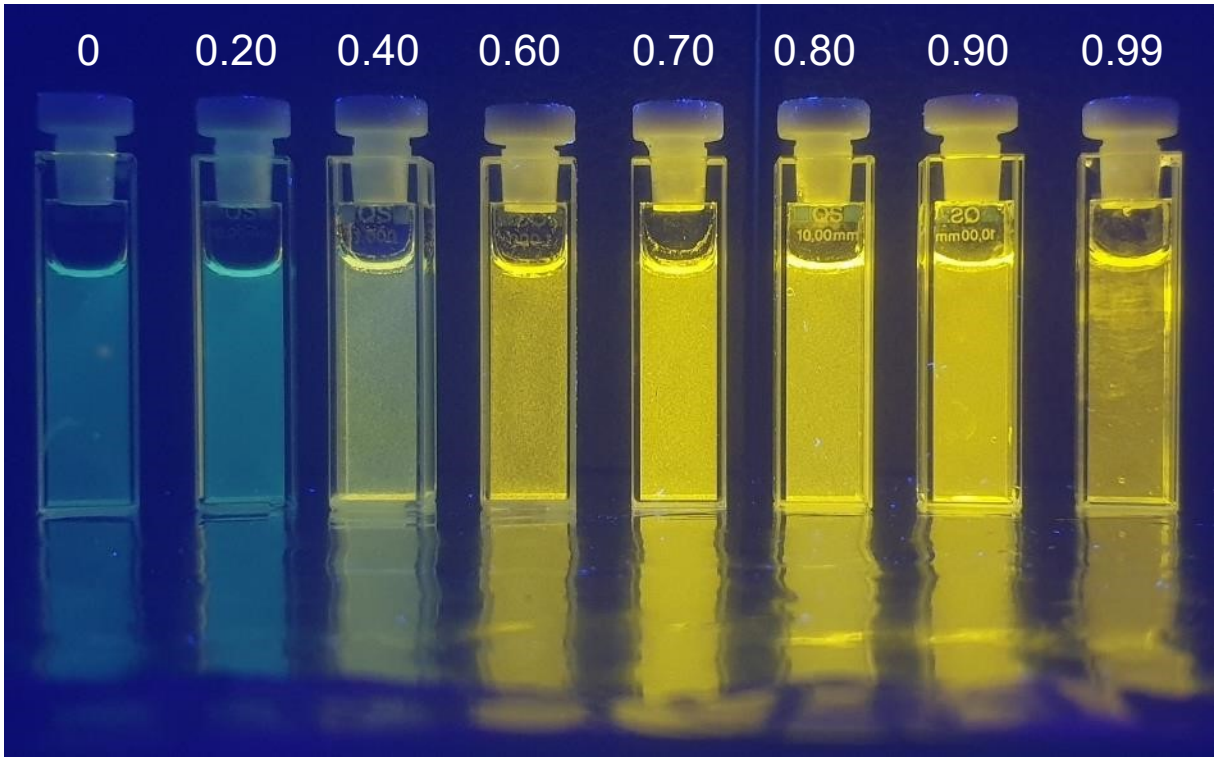

Fig. S21. Photograph of solutions of **2g** (2.0×10^{-5} mol/L) in water/acetonitrile with water fractions f_W = 0 – 0.99 under 366 nm UV irradiation.

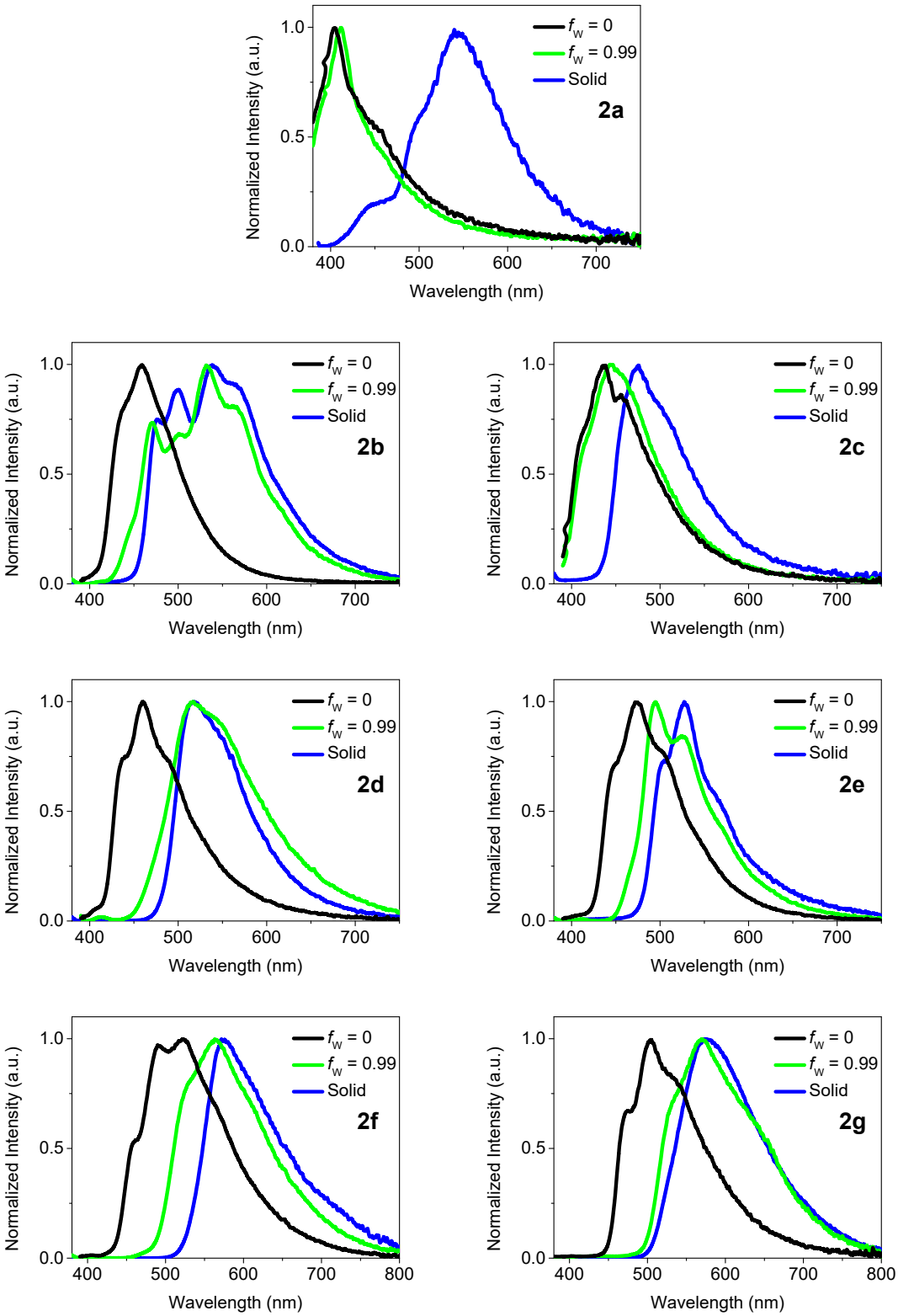

Fig. S22. Normalized emission spectra of **2a**-**2g** in solid state and solved in water/acetonitrile with water fractions f_w = 0 and 0.99, excited at 360 nm.

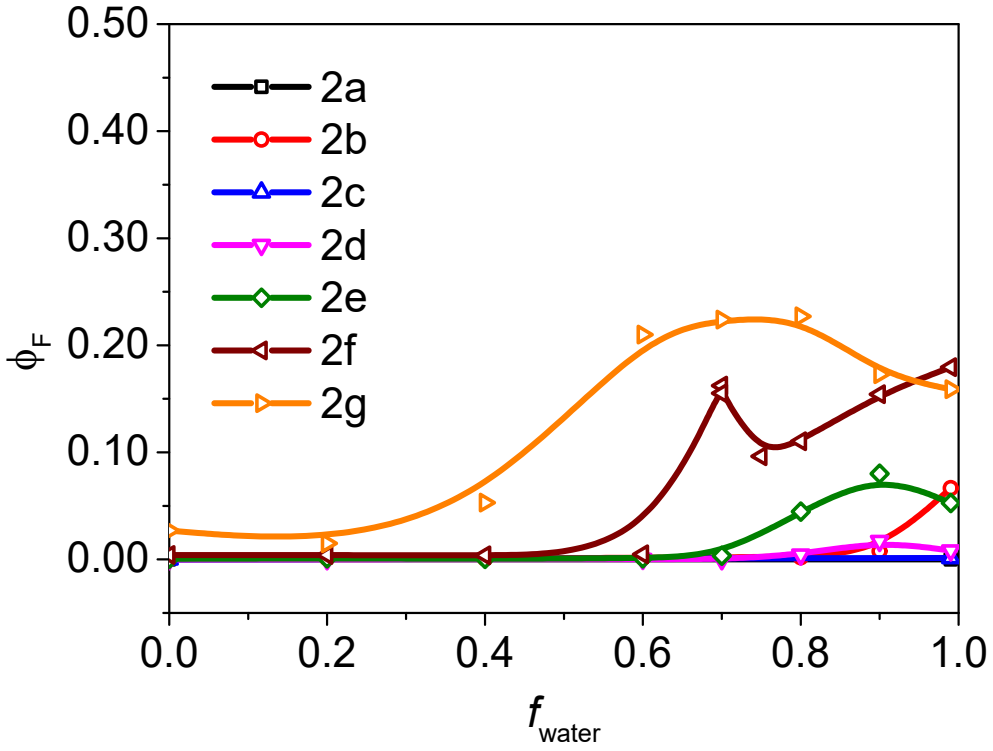

Fig. S23. Absolute fluorescence quantum yield ϕ_F of **2a-2g** versus water fraction f_W in water/acetonitrile mixtures, excited at 360 nm.

5. Time-Resolved Spectroscopy

5.1. Time-Correlated Single Photon Counting

Table S5. Decay fitting parameters of **2a**-**2g** in solid state and solved in water/acetonitrile with water fractions f_w = 0 and 0.99, excited at 360 nm and detected at 530 nm, measured with time correlated single photon counting.

Solvent	Molecule	τ_1 (ns)	A_1 (%)	τ_2 (ns)	A_2 (%)	τ_3 (ns)	A_3 (%)
Acetonitrile (f_w= 0)	**2a**	< 0.04	99.62	1.63	0.19	8.84	0.19
	2b (RT)	< 0.04	100				
	2b (77K)			0.50	39.25	2.95	60.75
	2c	< 0.04	100				
	2d	< 0.04	100				
	2e	< 0.04	100				
	2f	< 0.04	93.13	0.26	6.39	0.97	0.48
	2g	0.08	98.03	0.81	1.97		
Water/ acetonitrile mixture (f_w= 0.99)	**2a**	< 0.04	99.60	0.73	0.27	4.67	0.12
	2b	< 0.04	98.12	1.72	1.10	3.64	0.78
	2c	< 0.04	97.38	0.56	2.42	3.15	0.20
	2d	0.13	79.94	0.50	18.80	1.75	1.26
	2e	0.14	58.99	0.48	38.42	1.92	2.59
	2f	0.24	34.44	0.95	41.06	2.29	24.50
	2g	0.11	30.58	0.80	24.25	1.67	45.17
Solid state	**2a**	0.42	34.70	2.12	47.15	4.58	18.15
	2b			2.46	85.01	4.71	14.99
	2c	0.09	96.74	0.67	2.12	2.60	1.14
	2d			0.64	57.00	1.18	43.00
	2e			0.83	91.36	1.73	8.64
	2f			0.69	35.66	2.20	64.34
	2g			0.66	16.60	1.52	83.40

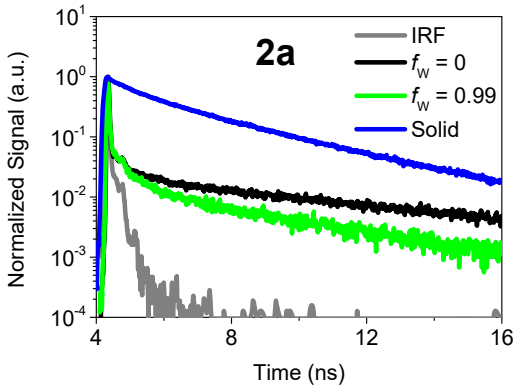
2a
IRF
f_w = 0
f_w = 0.99
Solid
Normalized Signal (a.u.)
Time (ns)

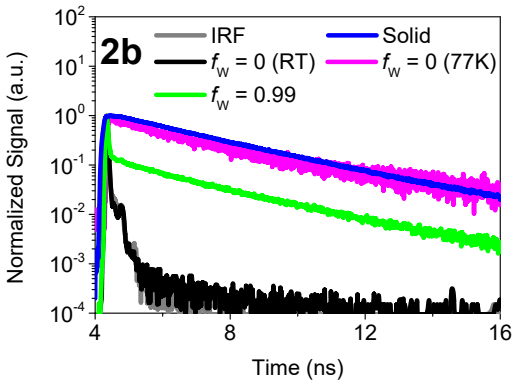
2b
IRF
f_w = 0 (RT)
f_w = 0.99
Solid
f_w = 0 (77K)
Normalized Signal (a.u.)
Time (ns)

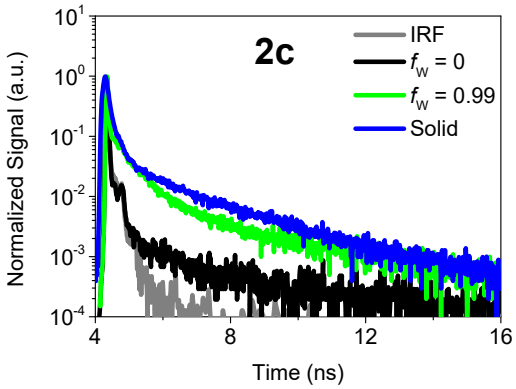
2c
IRF
f_w = 0
f_w = 0.99
Solid
Normalized Signal (a.u.)
Time (ns)

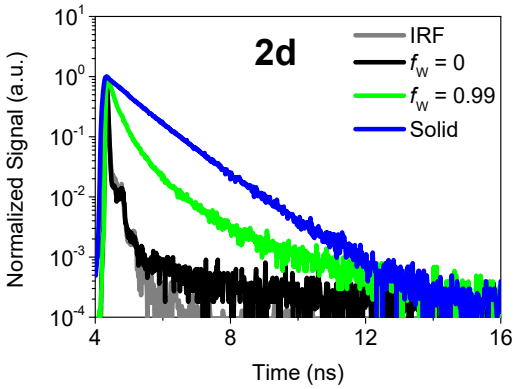
2d
IRF
f_w = 0
f_w = 0.99
Solid
Normalized Signal (a.u.)
Time (ns)

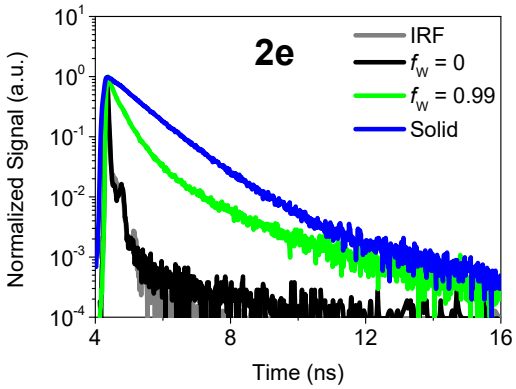
2e
IRF
f_w = 0
f_w = 0.99
Solid
Normalized Signal (a.u.)
Time (ns)

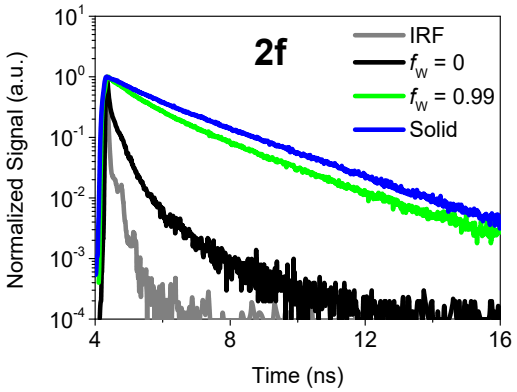
2f
IRF
f_w = 0
f_w = 0.99
Solid
Normalized Signal (a.u.)
Time (ns)

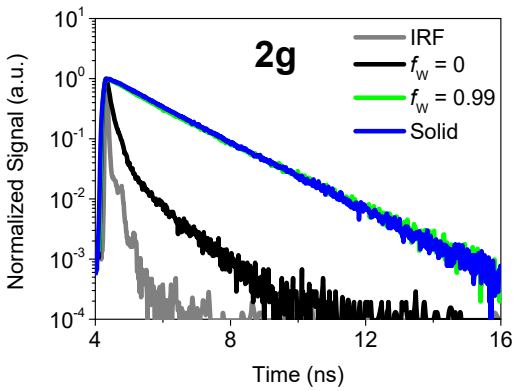
2g
IRF
f_w = 0
f_w = 0.99
Solid
Normalized Signal (a.u.)
Time (ns)

Fig. S24. Normalized fluorescence decays of **2a**-**2g** in solid state and solved in water/acetonitrile with water fractions f_w = 0 and 0.99, excited at 360 nm and detected at 530 nm, measured with time correlated single photon counting.

5.2. Femtosecond Fluorescence Up-Conversion

Table S6. Decay fitting parameters of **2a**-**2g** in acetonitrile, excited at 360 nm and detected at different wavelengths, measured with femtosecond fluorescence up-conversion. Negative amplitude ^{A_i} denotes a rise component.

Solvent	Molecule	Detection wavelength (nm)	τ_1 (ps)	A_1 (%)	τ_2 (ps)	A_2 (%)	τ_3 (ps)	A_3 (%)
Acetonitrile (f_w= 0)	**2a**	490	<0.1	100	1.5	<0.1		
		510	0.67	-100	0.79	99	73	1
		530	<0.1	-100	2.0	100		
		550	24	19	1.2	81		
	2b	510	1.6	58	9.1	42		
		530	3.2	67	11	33		
		550	1.6	61	8.9	39		
		570	8.9	43	1.9	57		
		590	15	31	2.5	69		
	2c	510	0.92	92	4.4	4	64	4
		530	1.0	-100	1.0	100	35	<0.1
		550	0.23	42	1.3	49	35	9
		570	1.2	-100	1.2	99	35	1
	2d	510	<0.1	-100	2.8	100		
		530	<0.1	-100	2.4	100		
		550	<0.1	-100	2.2	96	310	4
		570	<0.1	-100	1.9	21	50	79
		590	<0.1	-100	24	43	3.6	57
	2e	510	1.9	54	24	46		
		530	2.5	27	11	73		
		550	2.3	44	45	56		
	2f	510	0.45	-100	8.0	99	120	1
		530	0.34	-100	8.0	96	120	4
		550	0.45	-100	8.0	96	120	4
		570	0.45	-100	8.0	84	120	16
	2g	530	0.42	-100	8.7	54	61	46

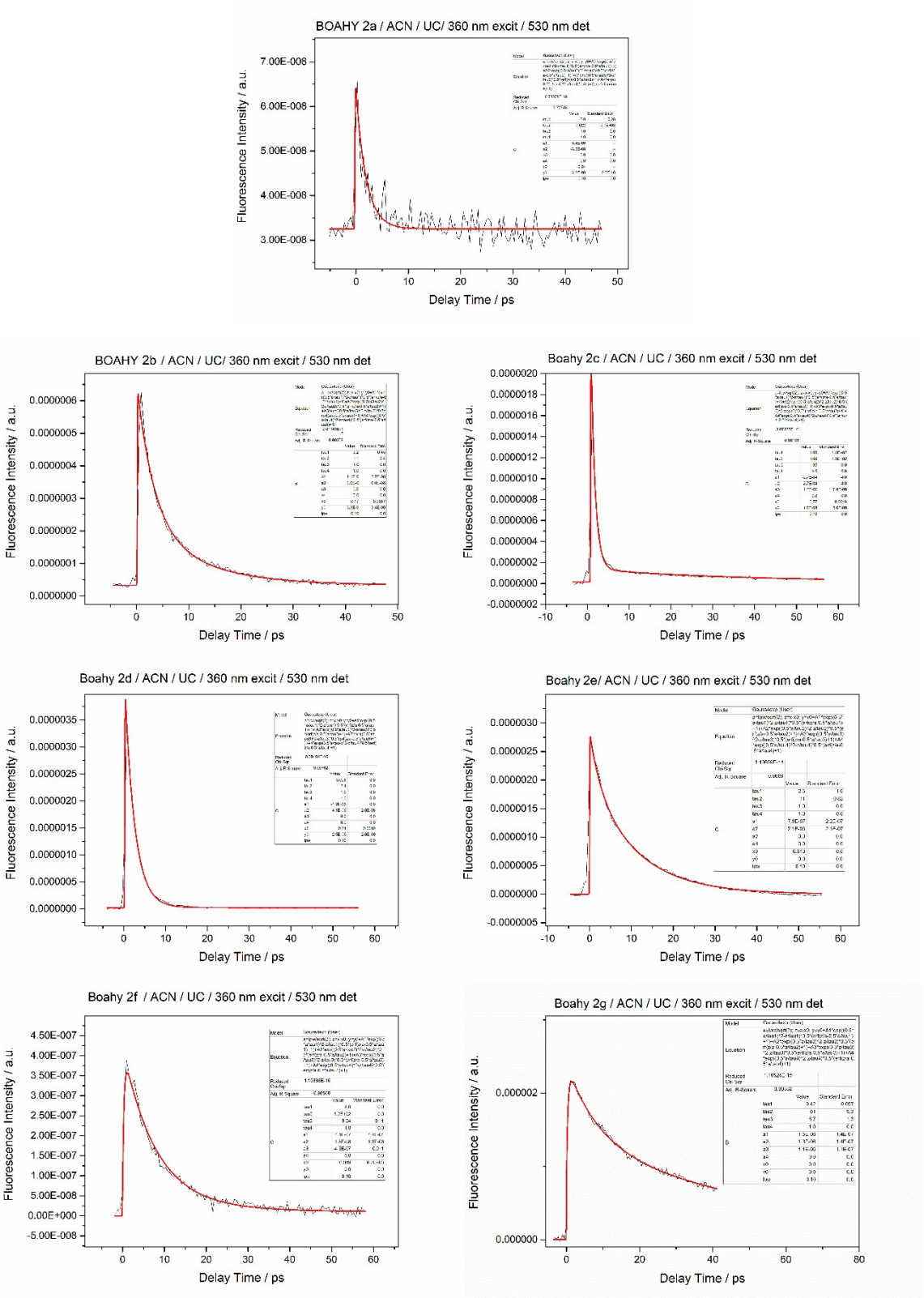

Fig. S25. Fluorescence decays of **2a**-**2g** (2.0×10^{-5} mol/L) in acetonitrile, excited at 360 nm and detected at 530 nm, measured with femtosecond fluorescence upconversion.

6. Fluorescence Microscopy

BOAHY dye 2f in aqueous medium

BOAHY testing was performed in a 29 mm disk containing a 14 mm glass bottom insert that allows for high resolution imaging (Cellvis, D29-14-1.5-N). BOAHY dye **2f** was diluted to a concentration of 10 µmol/L in a total volume of 2 mL cell culture medium, which was prepared by adding 2 µL of a 10 mmol/L stock solution of the BOAHY dye in DMSO to 2 mL cell culture medium. The sample was incubated for approximately 15 minutes at room temperature to allow dye to settle on the glass coverslip, and subsequently imaged in confocal microscopy.

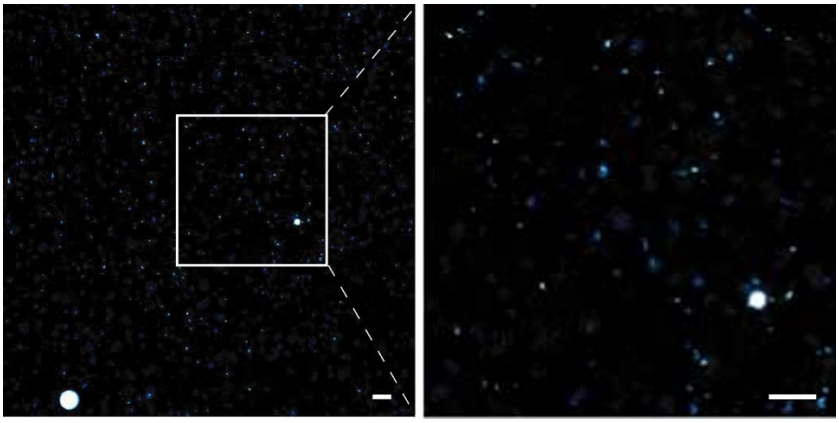

Fig. S26. Fluorescence microscopy image BOAHY dye **2f** (cyan) in aqueous medium. Scale bars 10 µm.

BOAHY dye 2f compatibility with mammalian cells: cell culture and stainings

HeLa cells were purchased from ATCC (American Type Culture Collection) and maintained under standard cell culture conditions at 37°C in a humidified incubator with 5% CO_2 supplemented. Cells were grown in cell culture medium consisting of Dulbecco's Modified Eagle Medium (DMEM, Gibco) supplemented with 10% Fetal Bovine Serum (FBS, Sigma), 1% GlutaMAX (Gibco) and 0.1% Gentamycin (Carl Roth). For BOAHY testing, 400 000 HeLa cells were seeded in a 29 mm disk containing a 14 mm glass-bottom insert (Cellvis, D29-14-1.5-N) and grown for approximately 20 hours to reach ~ 90% confluency.

In case of lysosomal staining, cells were stained prior to addition of the BOAHY dye. Briefly, cells were washed 3x with 2 mL prewarmed DPBS 1x (Thermo) and incubated with 400 µL of the commercially available LysoTracker™ Deep Red dye (Thermo, L12492), which was diluted in DMEM (Gibco) supplemented with 1% GlutaMAX (Gibco) to obtain a final concentration of 50 nM. Incubation with LysoTracker™ Deep Red was performed for 45 minutes in the dark, under standard cell culture conditions. Afterwards, the staining solution was removed, cells were washed 3x with 2 mL prewarmed DPBS 1x (Thermo) and incubated in 2 mL cell culture medium.

For BOAHY testing, cells were washed 3x with 2 mL prewarmed DPBS 1x (Thermo) and incubated for 4 hours with 10 µmol/L BOAHY dye in a total volume of 2 mL cell culture medium, which was prepared by adding 2 µL of a 10 mmol/L stock solution of the BOAHY dye in DMSO to 2 mL cell culture medium. It has previously been shown that this concentration of DMSO has no effect on the cell growth and proliferation.[5] Afterwards, the BOAHY solution was removed, cells were washed 3x with 2 mL prewarmed DPBS 1x (Thermo), incubated in 2 mL prewarmed HBSS (Gibco) and taken for live-cell imaging either immediately or after membrane staining.

For membrane staining, cells were stained after incubation with the BOAHY dye. To this end, medium was removed and cells were washed 2x with 2 mL prewarmed DPBS 1x (Thermo). Cells were then incubated with 300 µL of the commercially available DiR dye (Thermo, D12731), which was diluted in HBSS (Gibco) to obtain a final concentration of 10 µg/mL. Incubation was performed for 15 minutes in the dark, under standard cell culture conditions. Afterwards, the cells were washed 3x with prewarmed DPBS and incubated in 2 mL HBSS for live-cell imaging.

Confocal imaging

Samples were imaged on a confocal Leica TCS SP8 microscope (Leica Microsystems GmbH) with 63x water (NA: 1.2) immersion objective. Samples were excited using a diode laser at 405 nm for the BOAHY dye, and at 638 nm for DiR or LysoTracker™ Deep Red. Highly sensitive hybrid detectors (HyD SMD, Leica Microsystems GmbH) captured emission between 500 - 635 nm for **2f**, and 643 – 780 nm for DiR or LysoTracker™ Deep Red. In parallel, transmission images were captured on a transmitted light detector. Image acquisition was performed at 512x512 pixels and 400 Hz line scan speed. Images were processed using ImageJ 1.53c.[6,7]

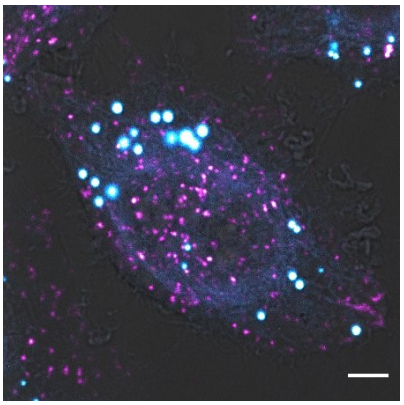

Fig. S27. Fluorescence microscopy image of a HeLa cell incubated with BOAHY dye **2f** (cyan) and stained with lysosomal LysoTracker™ Deep Red stain (pink). The figure displays the cross-section of a cell and overlay with the transmission image. Scale bar 5 µm.

7. NMR Spectroscopy

^{1}H NMR spectrum of 2a

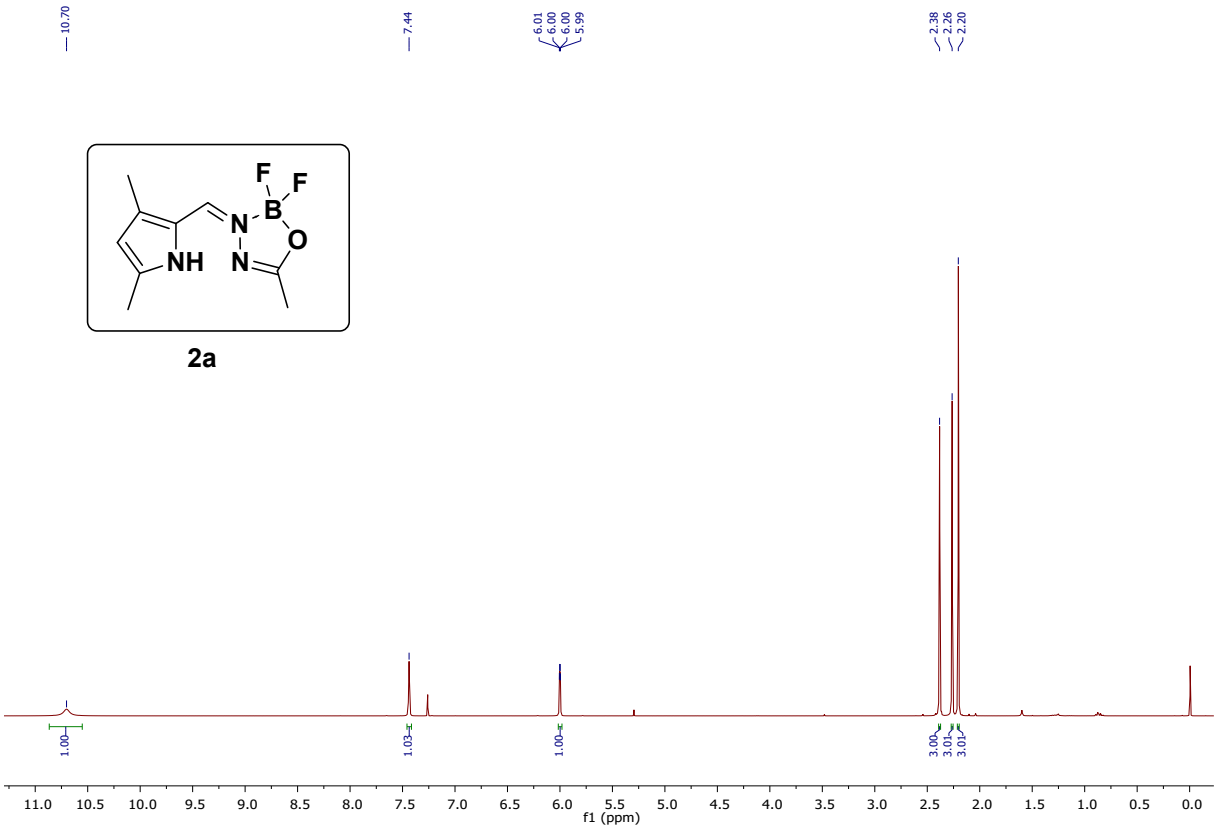

^{13}C NMR spectrum of 2a

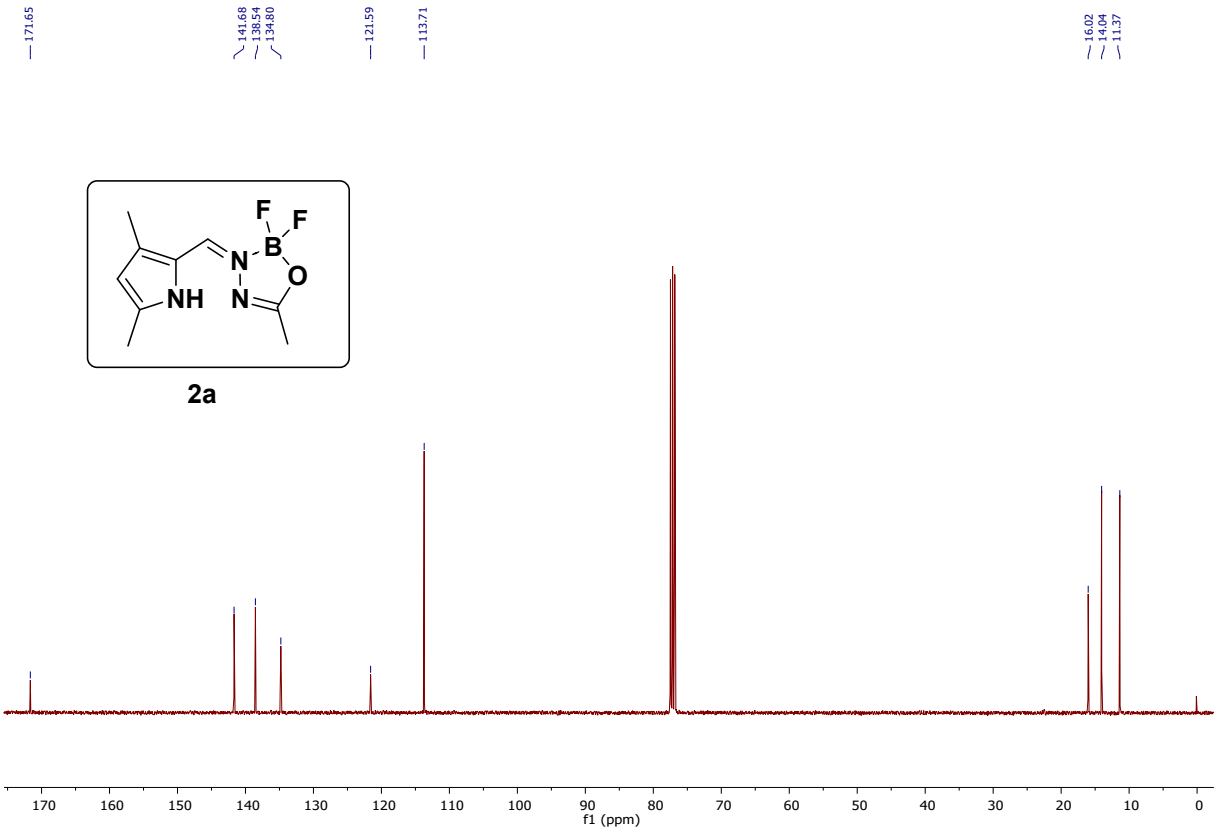

^{11}B NMR spectrum of 2a

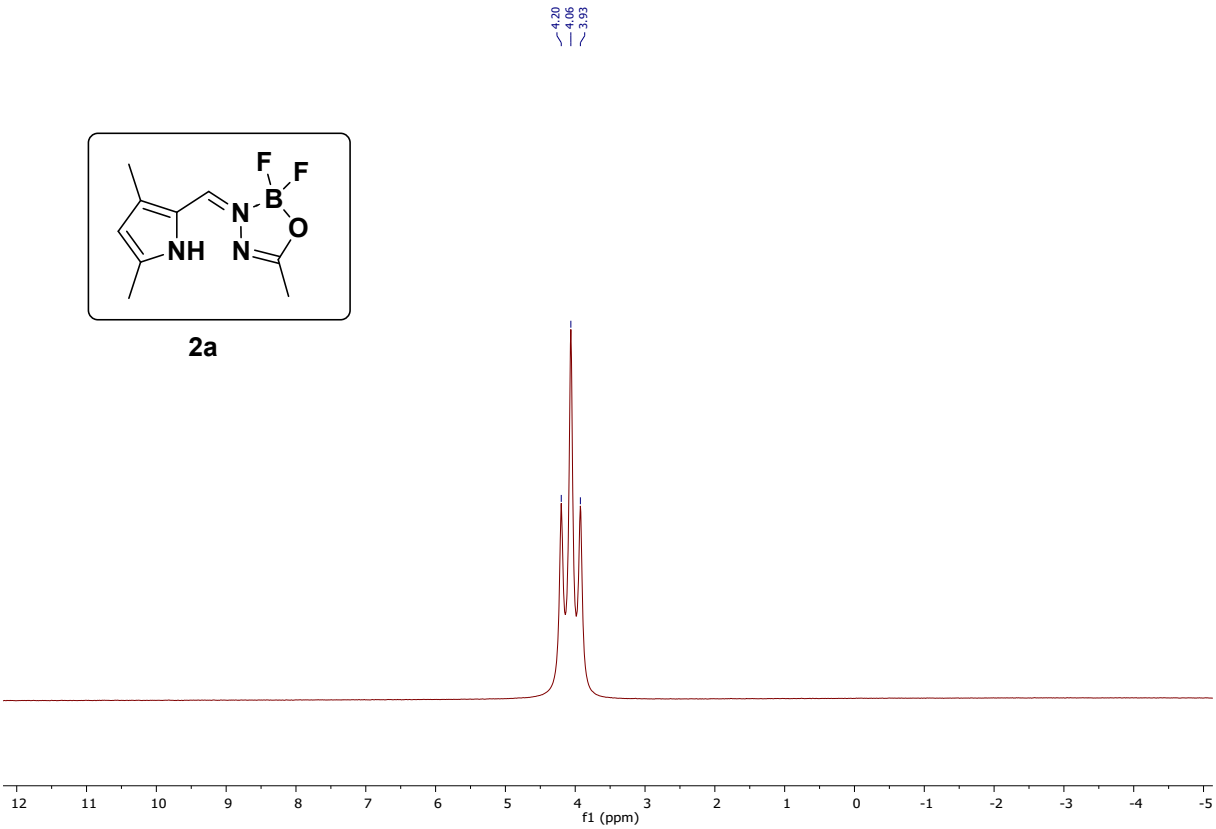

^{19}F NMR spectrum of 2a

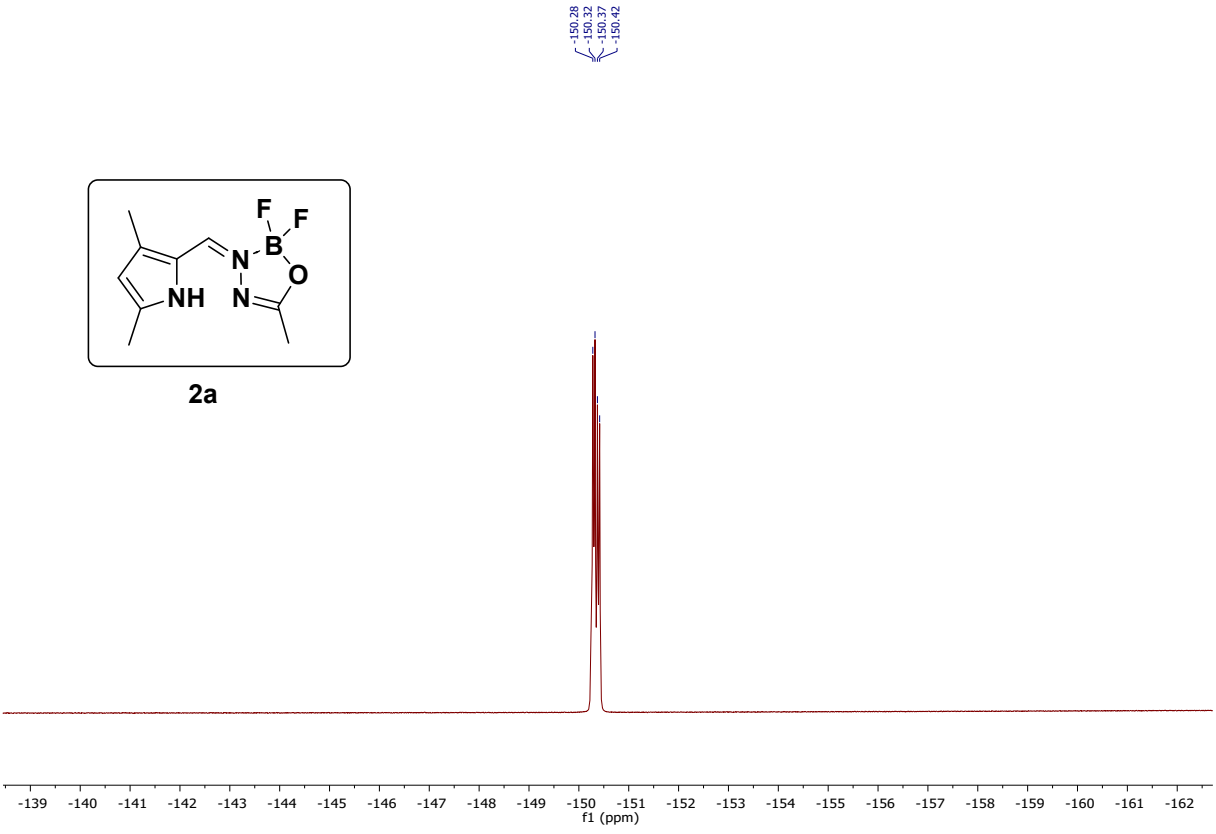

^{1}H NMR spectrum of 2b

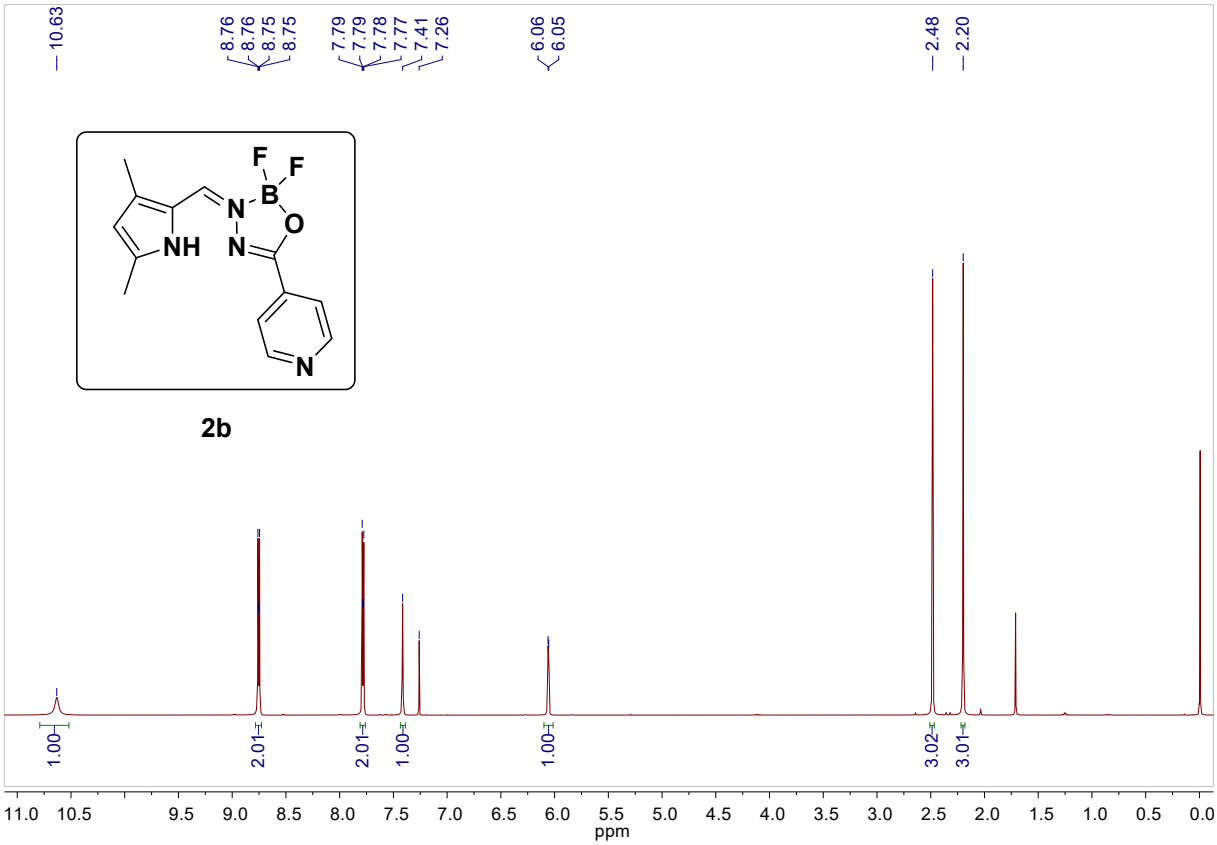

^{13}C NMR spectrum of 2b

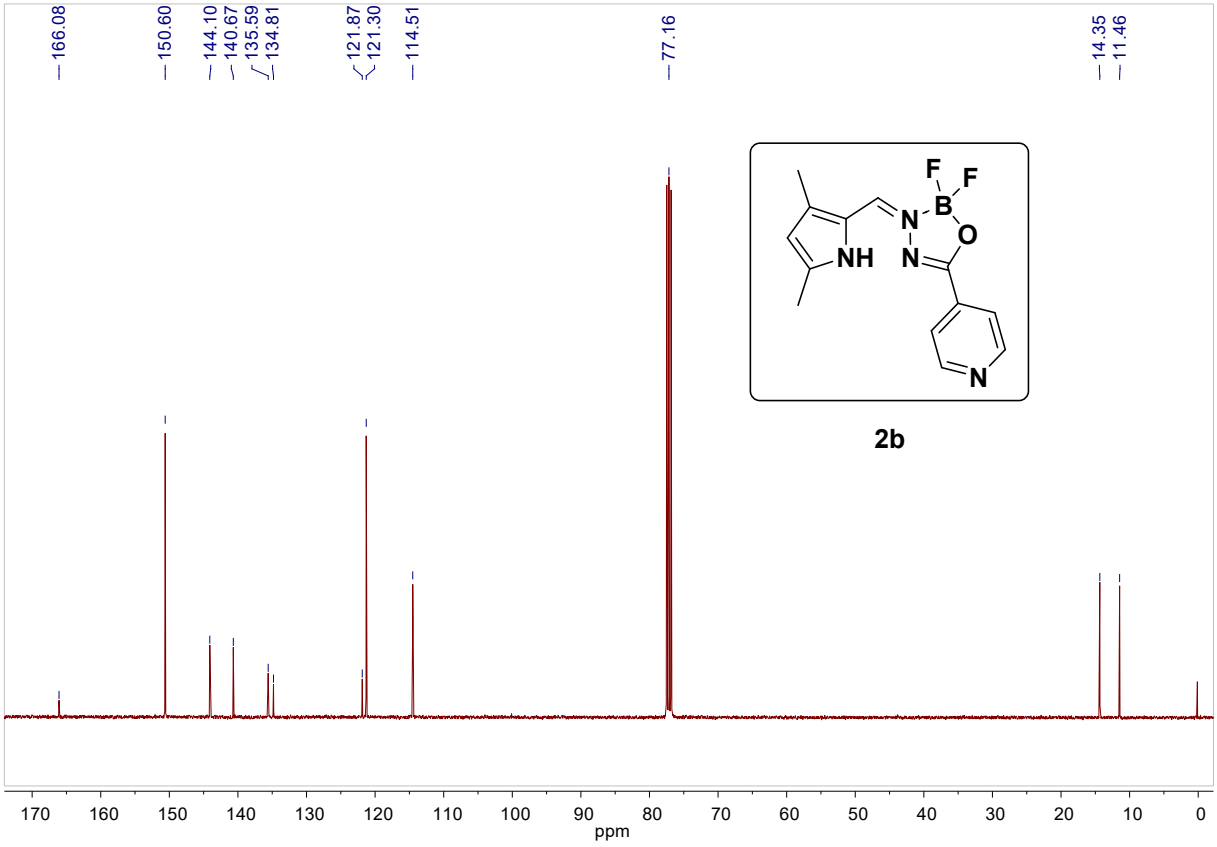

^{11}B NMR spectrum of 2b

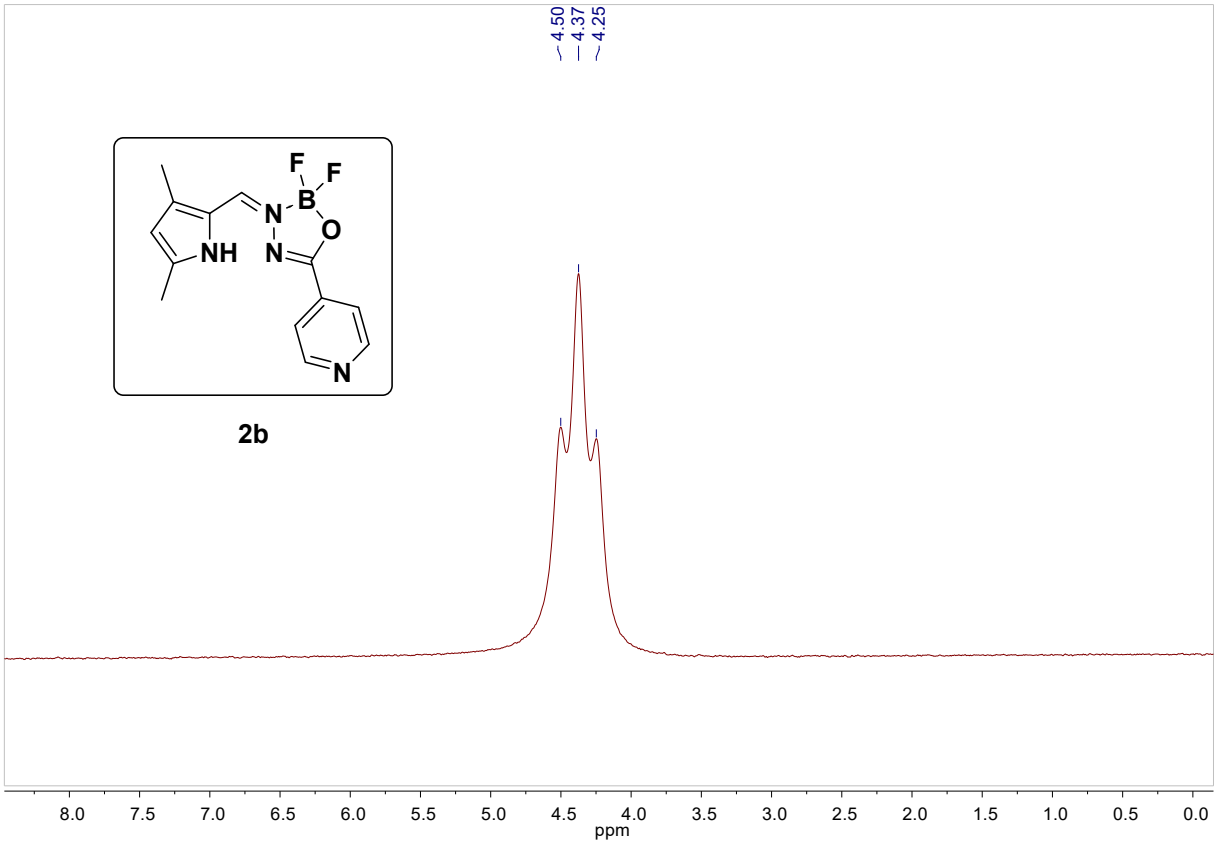

^{19}F NMR spectrum of 2b

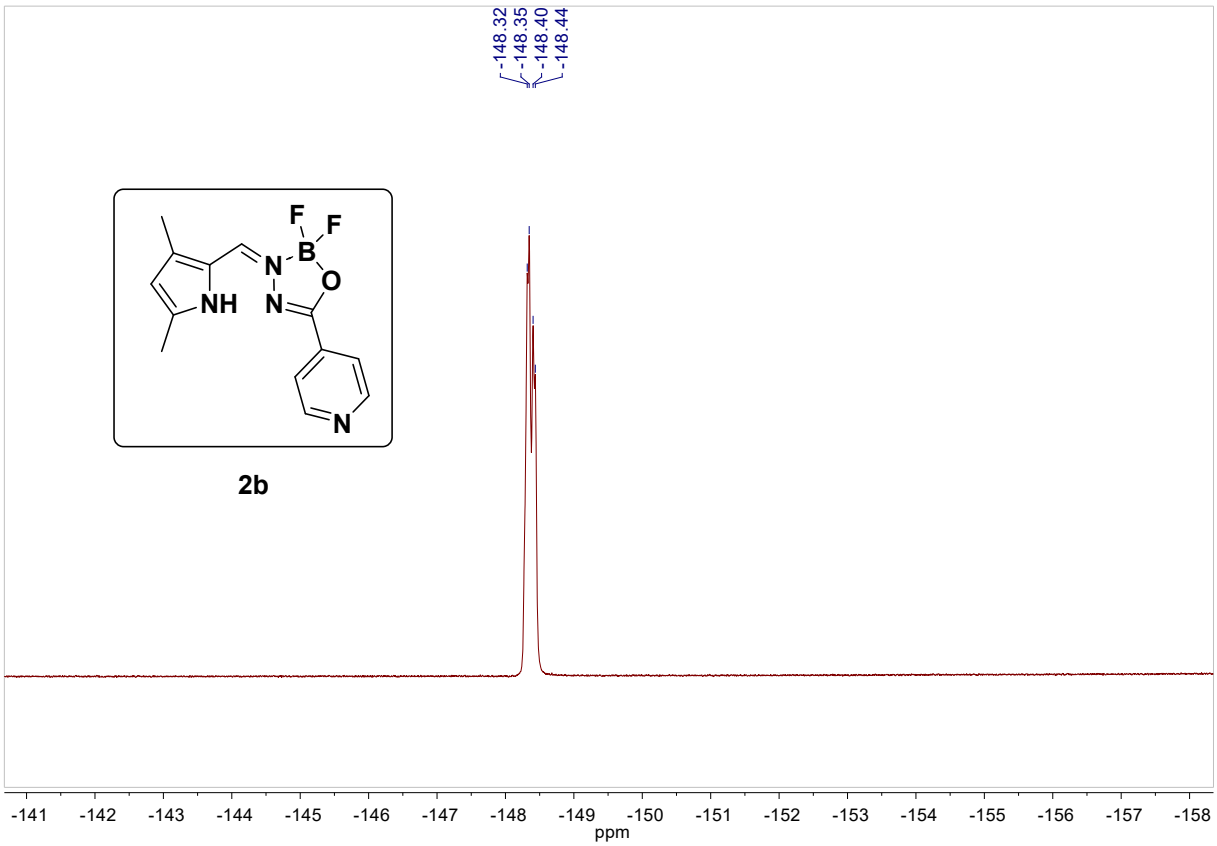

^{1}H NMR spectrum of 2c

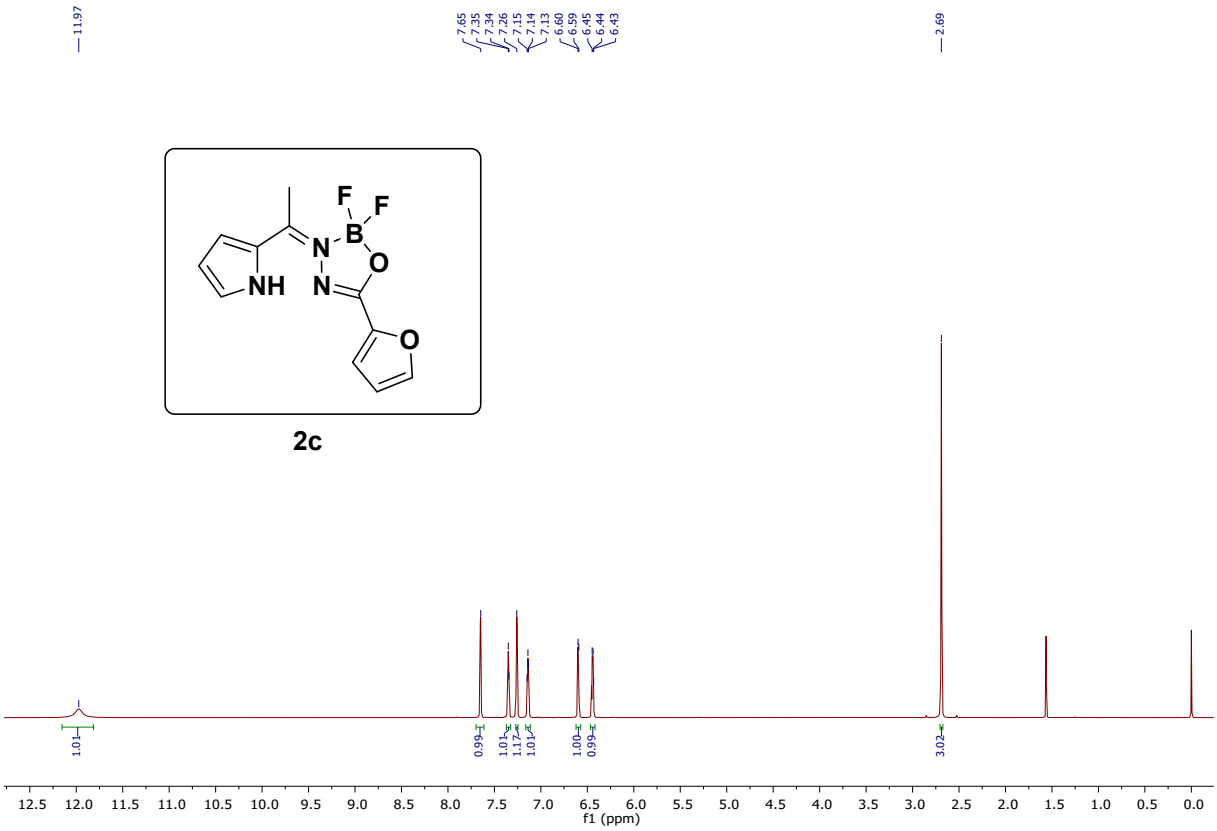

^{13}C NMR spectrum of 2c

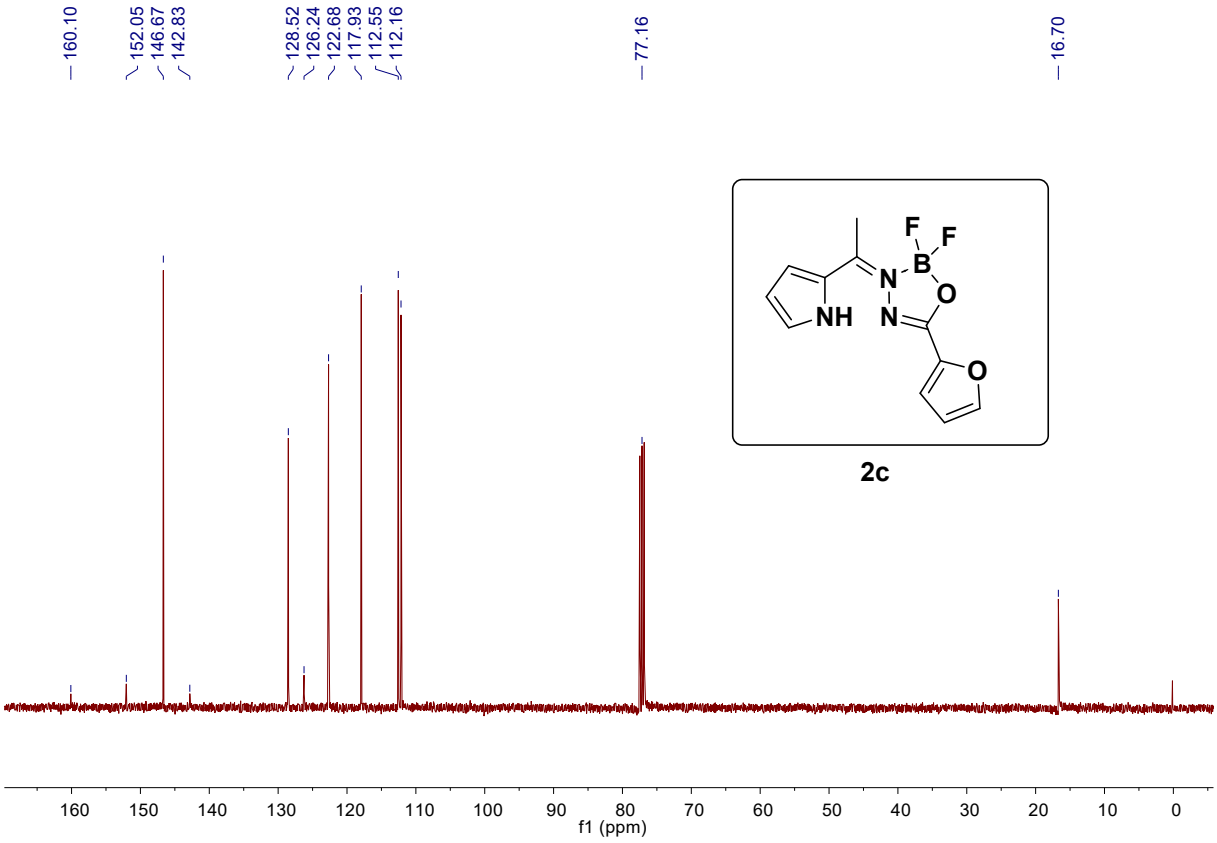

^{11}B NMR spectrum of 2c

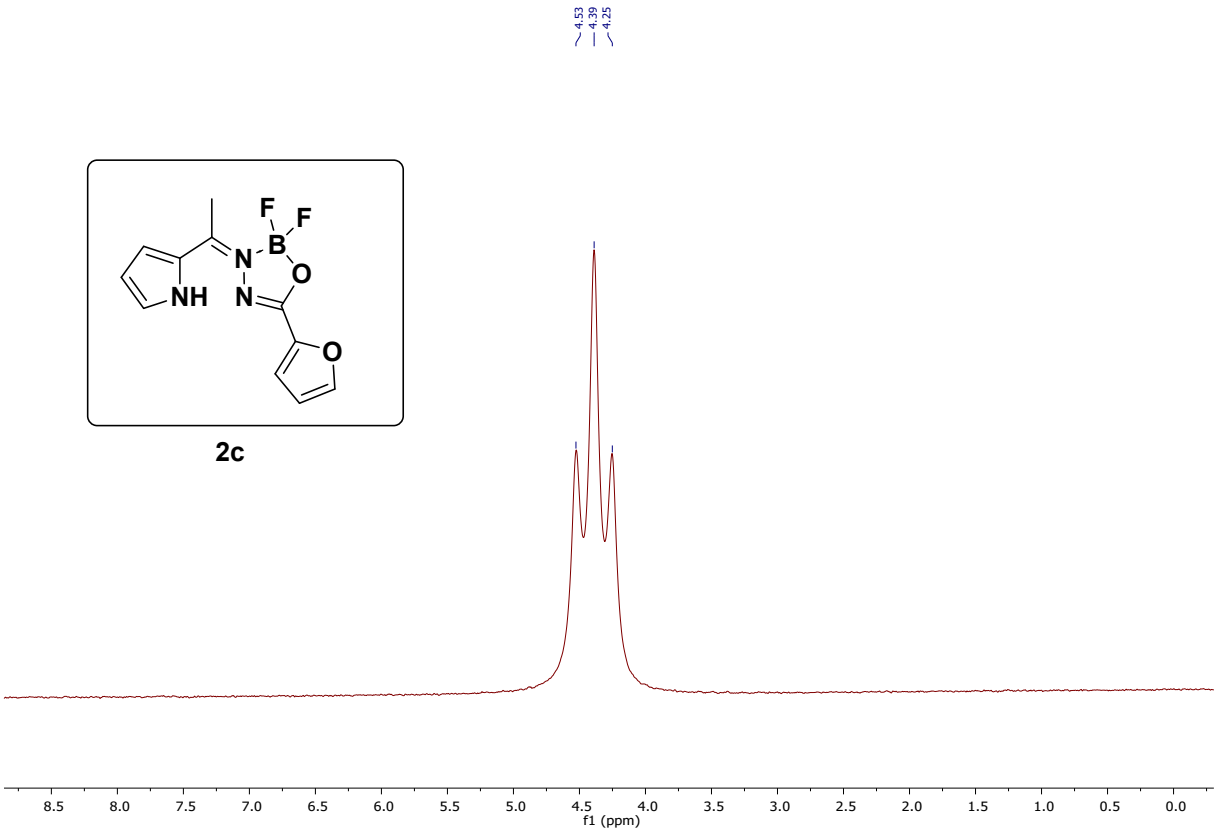

2c

^{19}F NMR spectrum of 2c

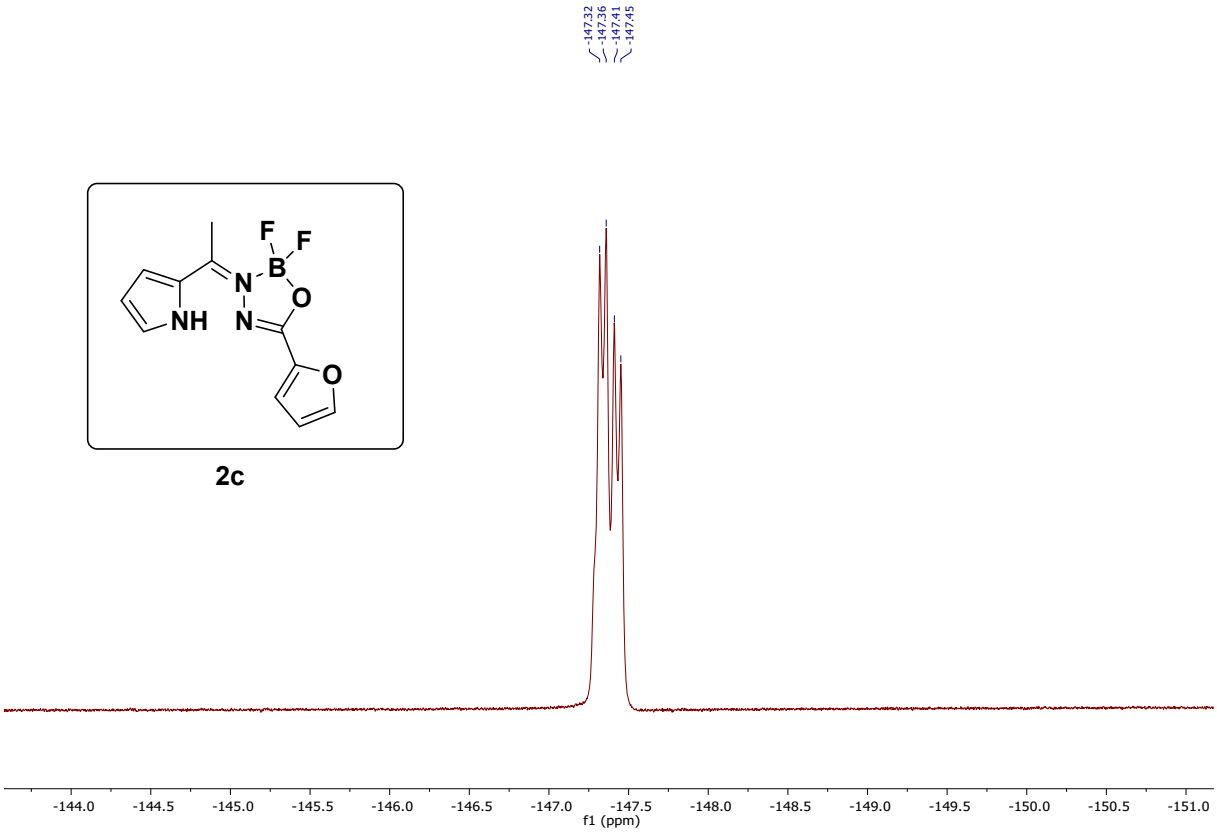

2c

^{1}H NMR spectrum of 2d

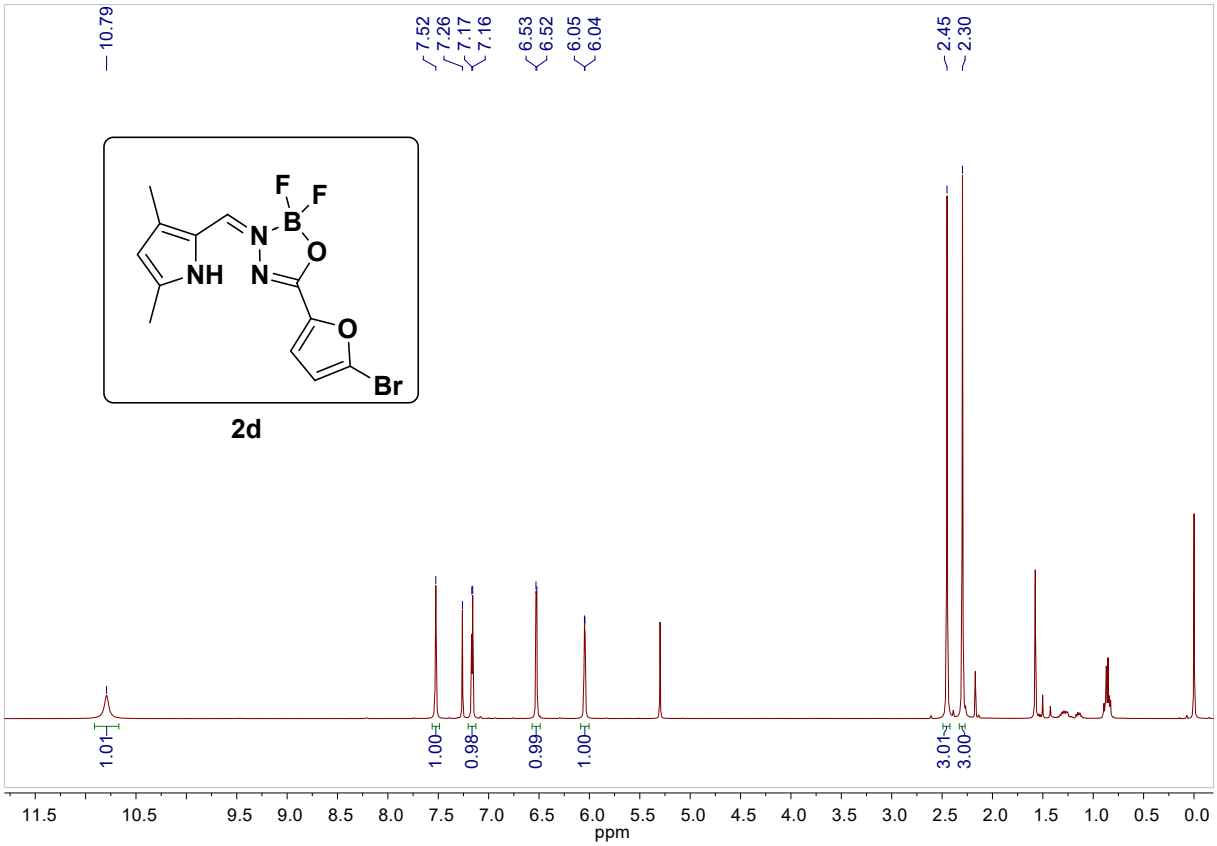

^{13}C NMR spectrum of 2d

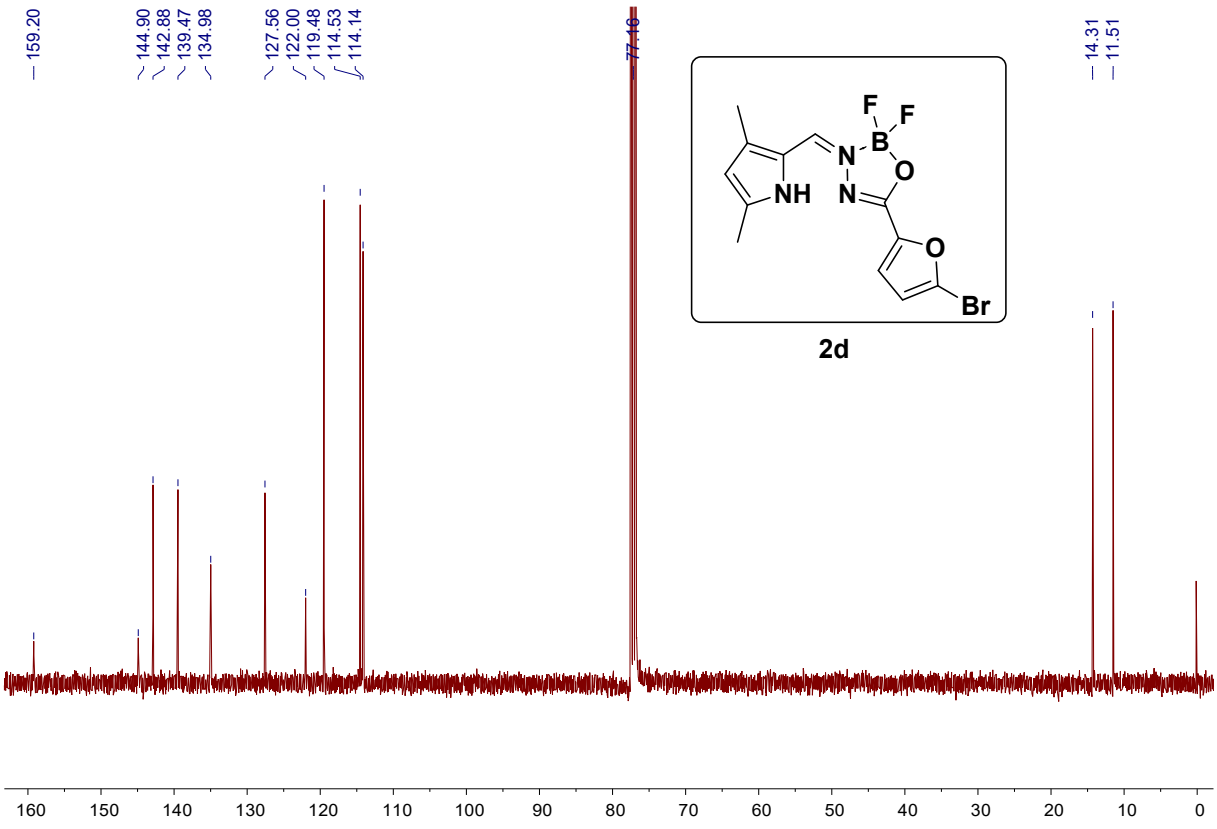

^{11}B NMR spectrum of 2d

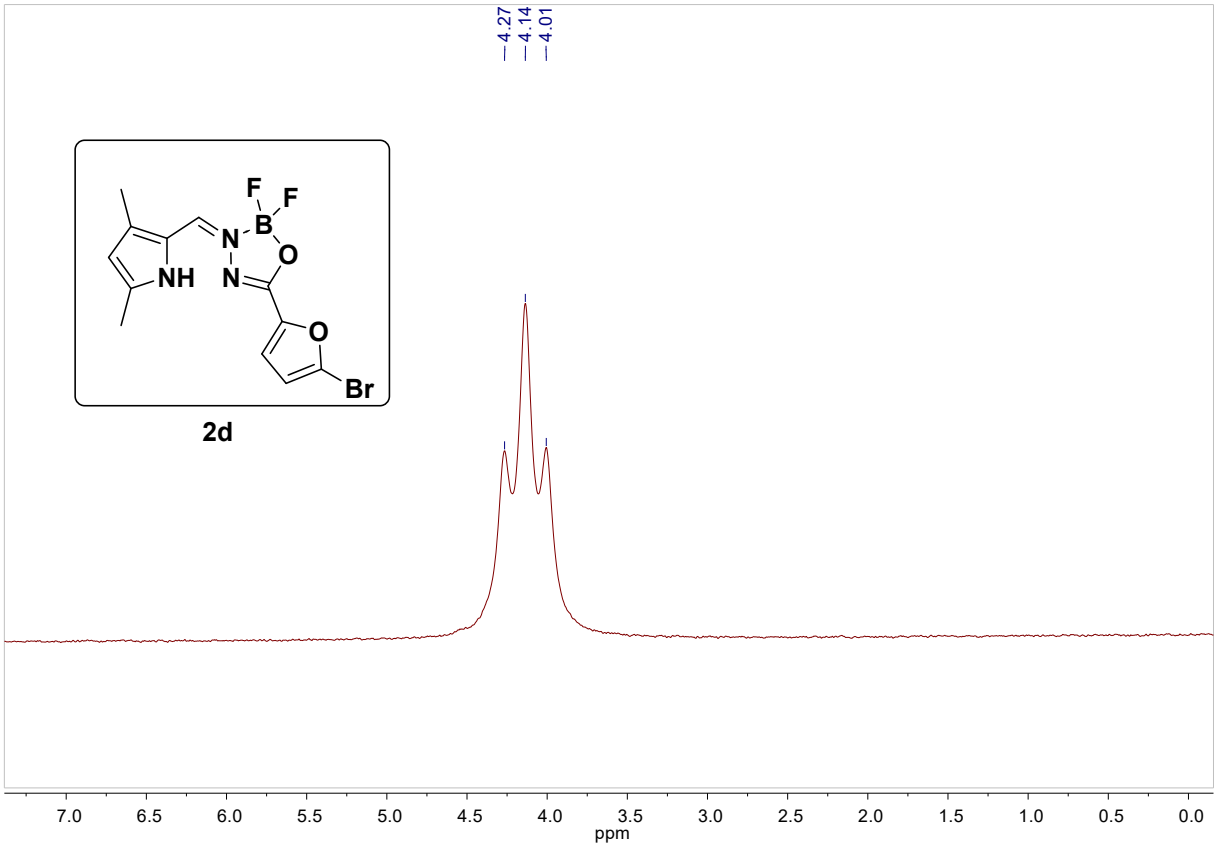

^{19}F NMR spectrum of 2d

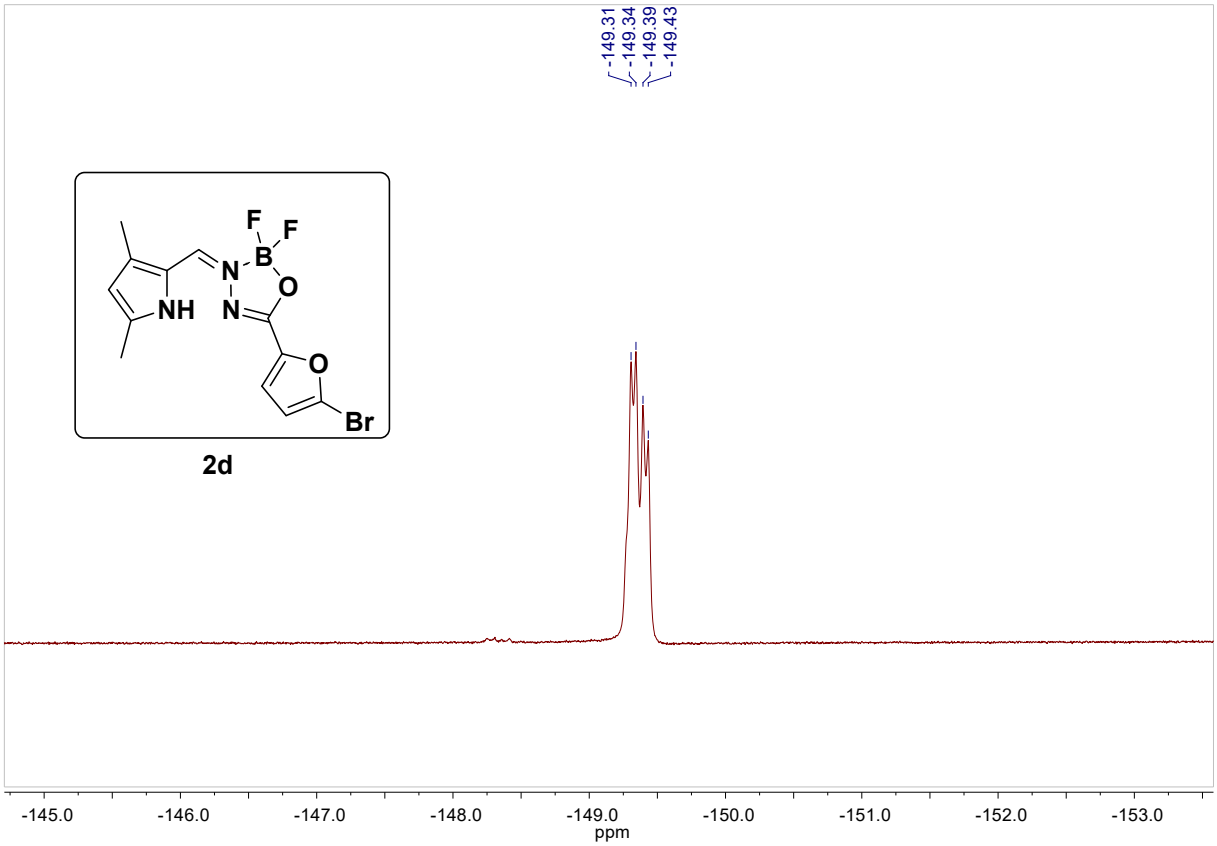

^{1}H NMR spectrum of 2e

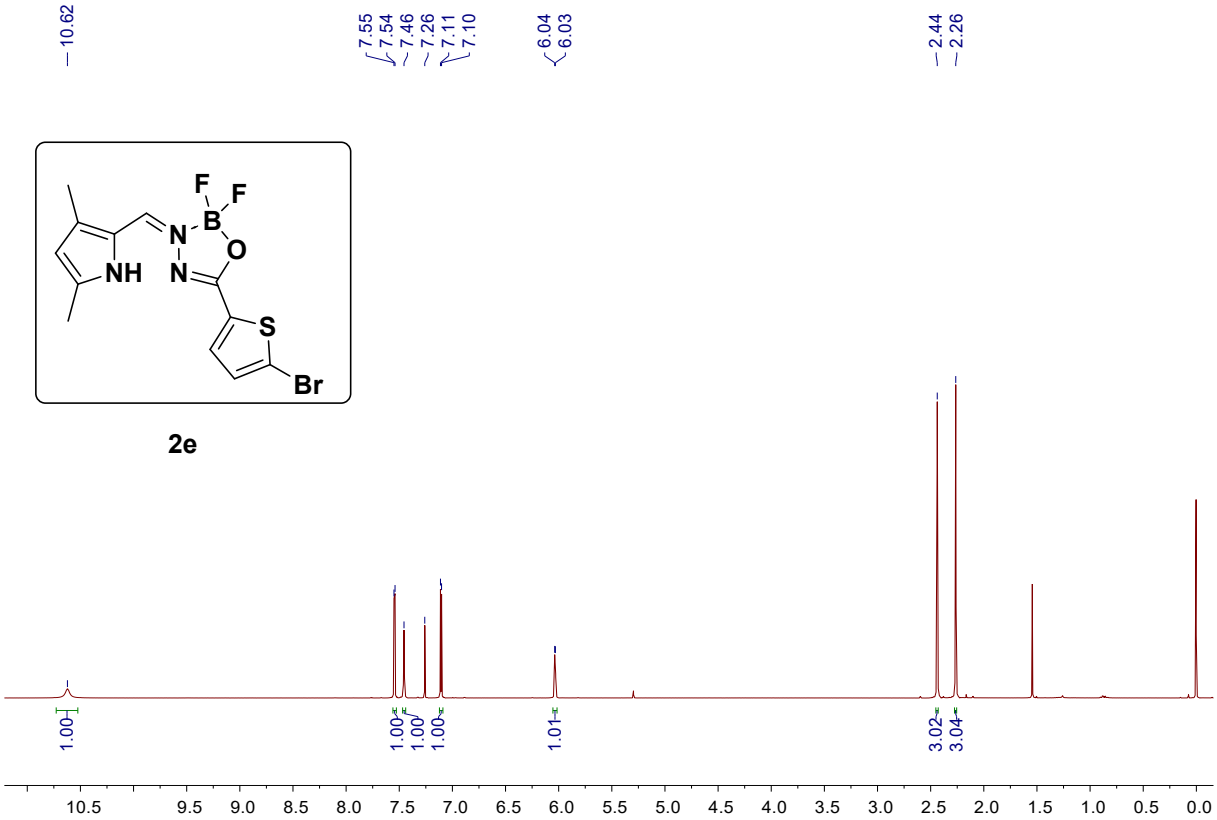

^{13}C NMR spectrum of 2e

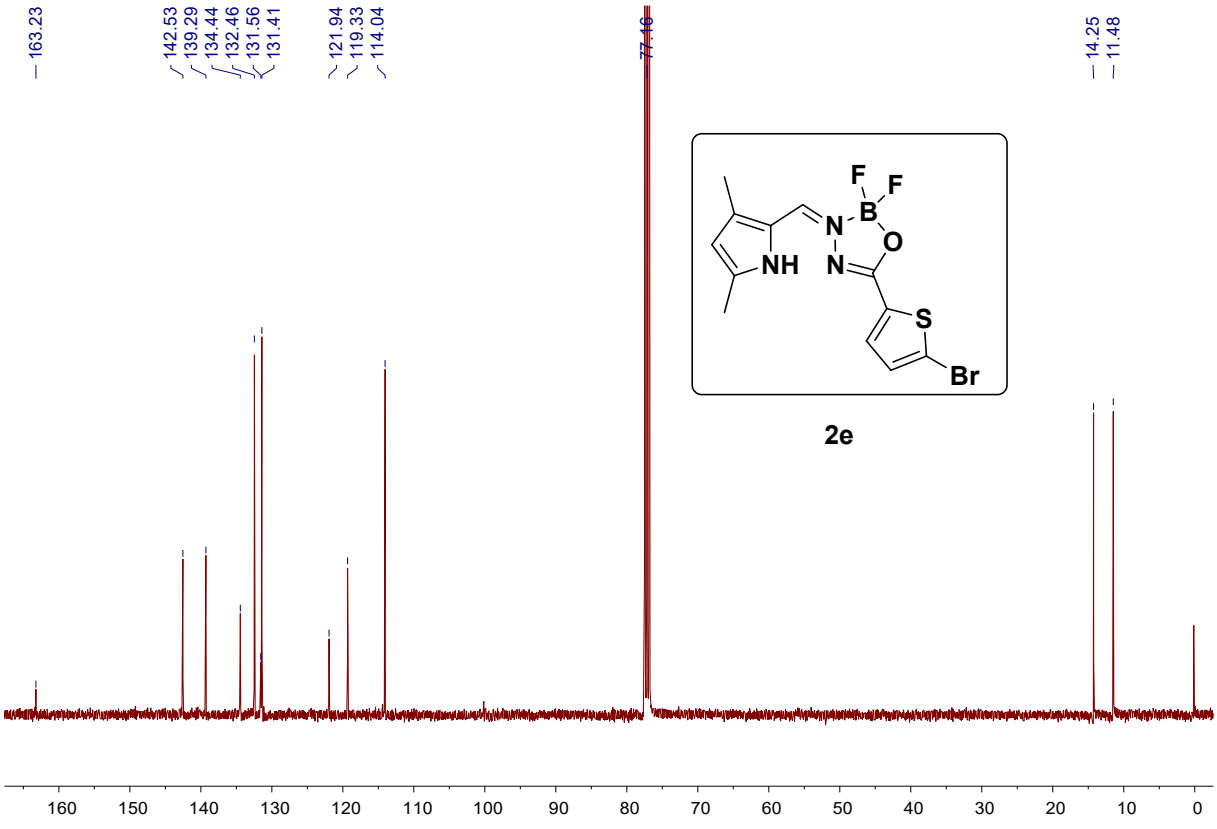

^{11}B NMR spectrum of 2e

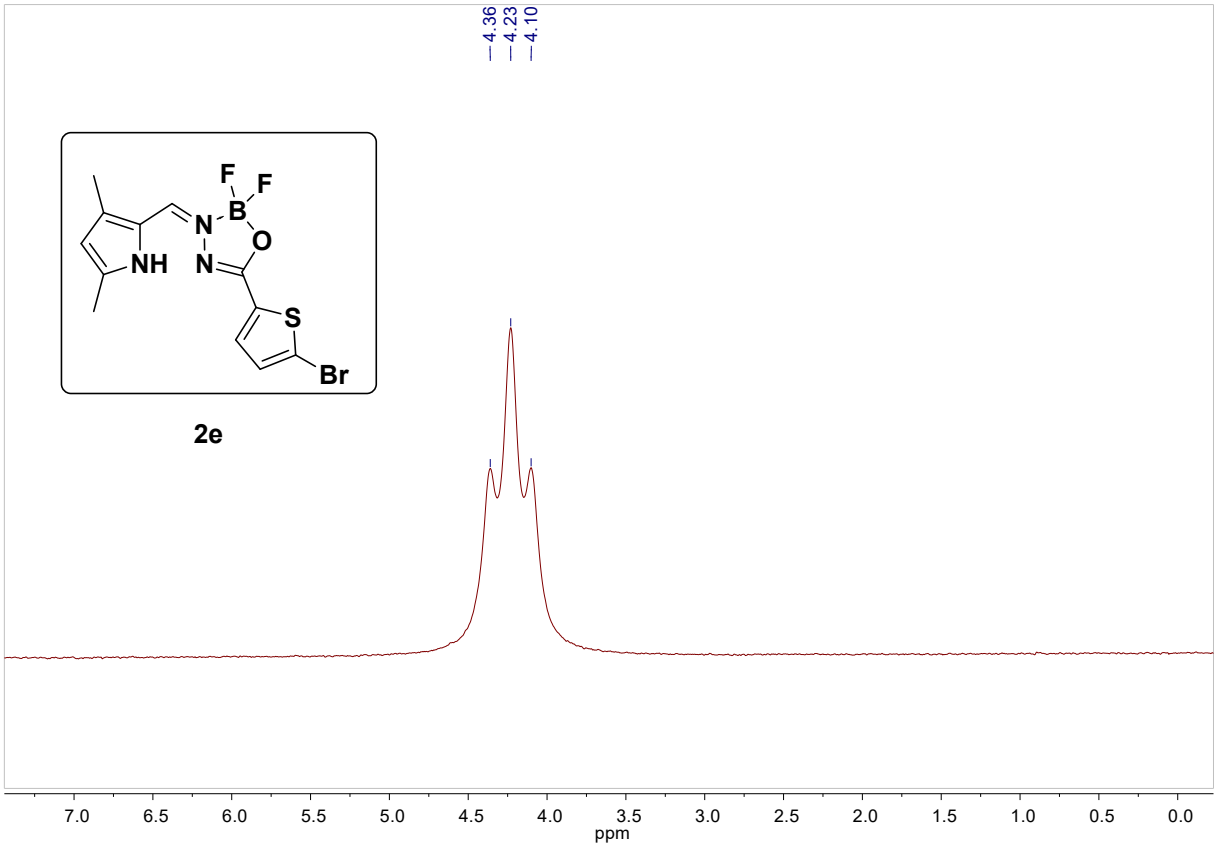

^{19}F NMR spectrum of 2e

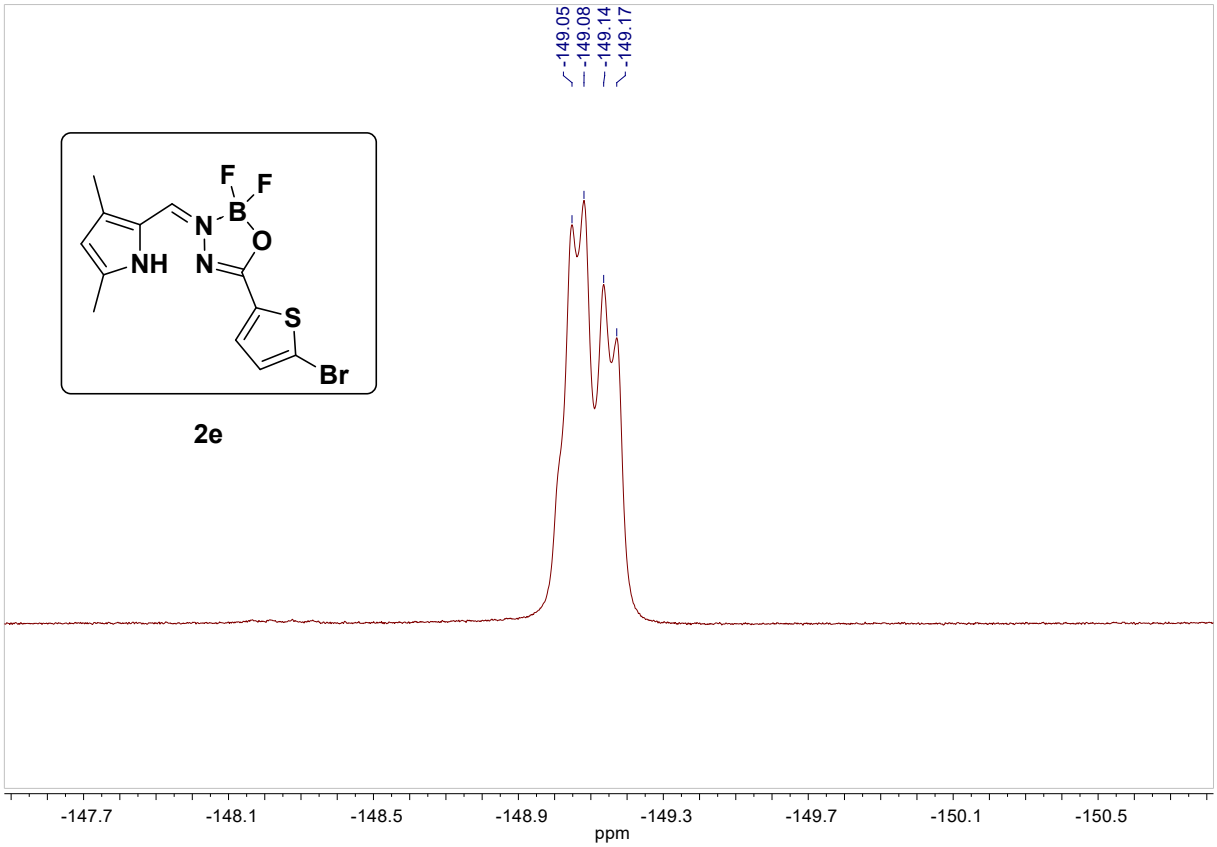

^{1}H NMR spectrum of 2f

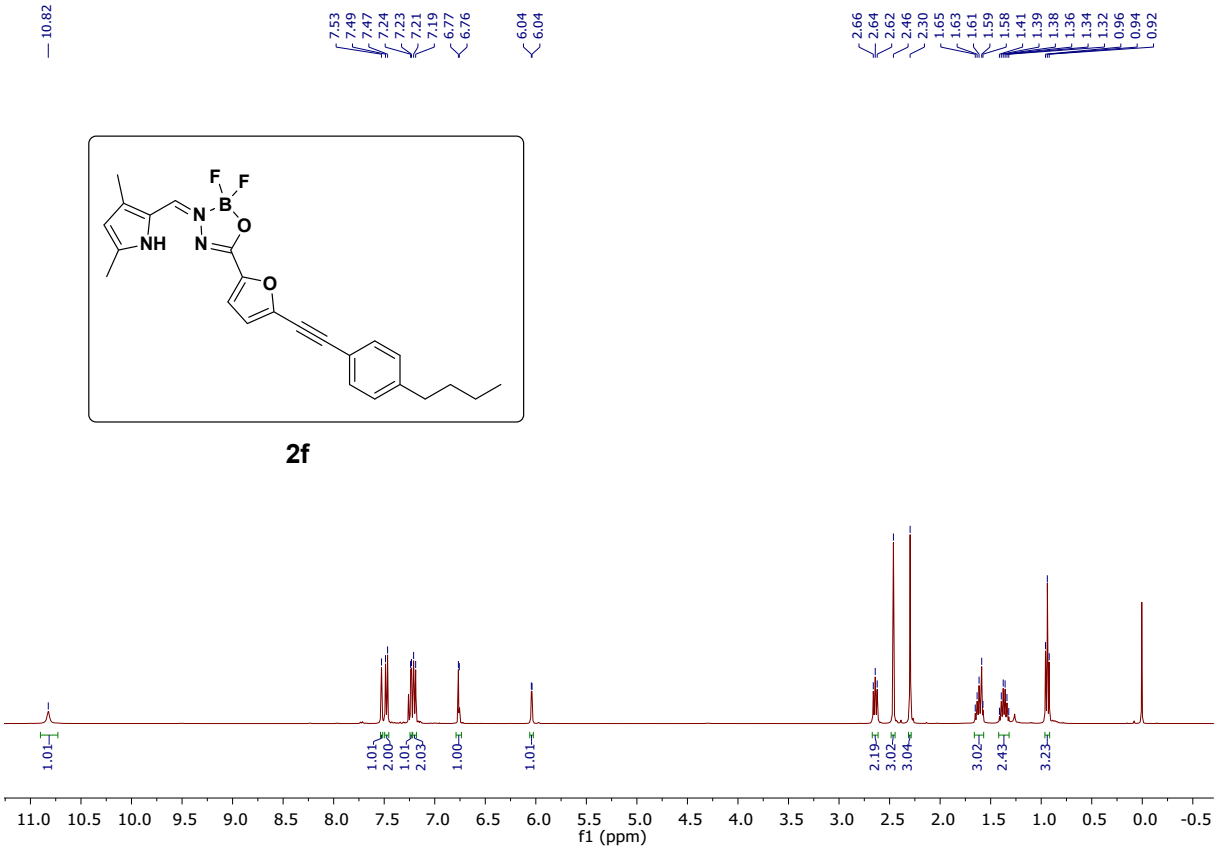

^{13}C NMR spectrum of 2f

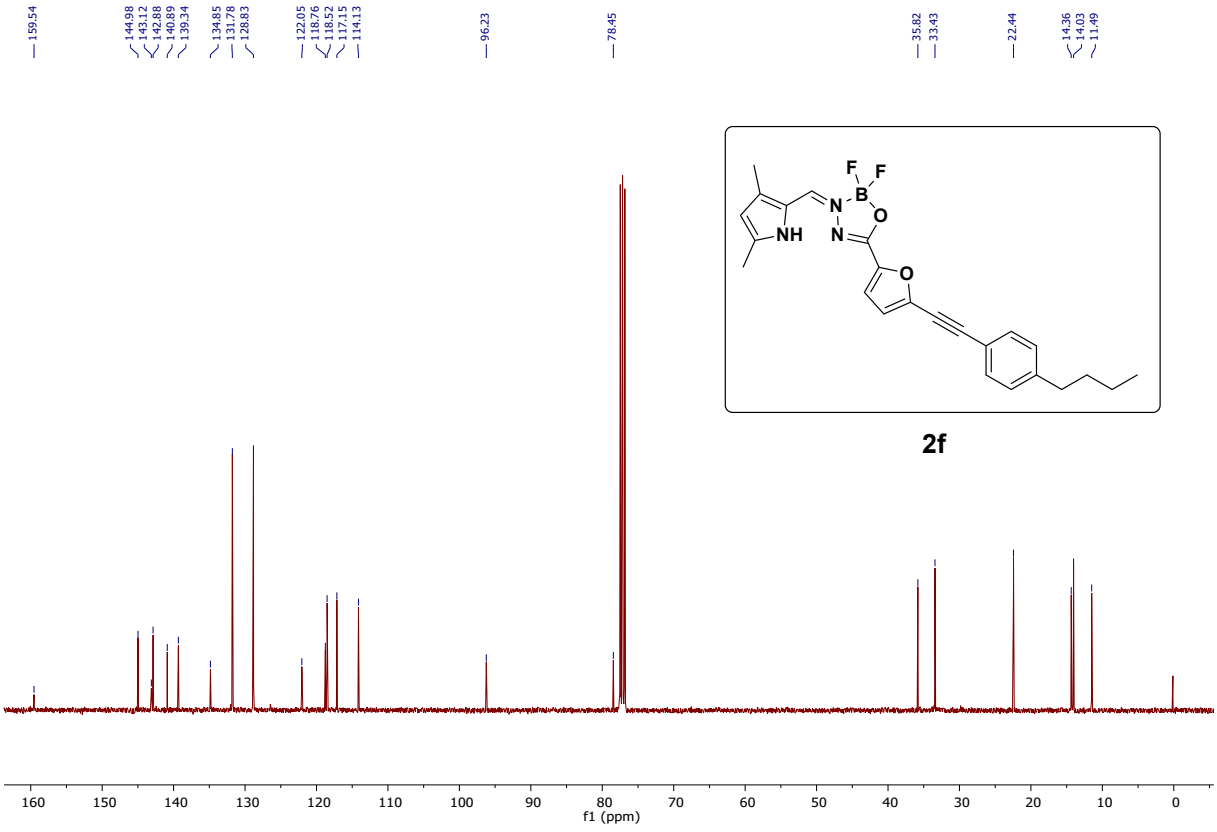

^{11}B NMR spectrum of 2f

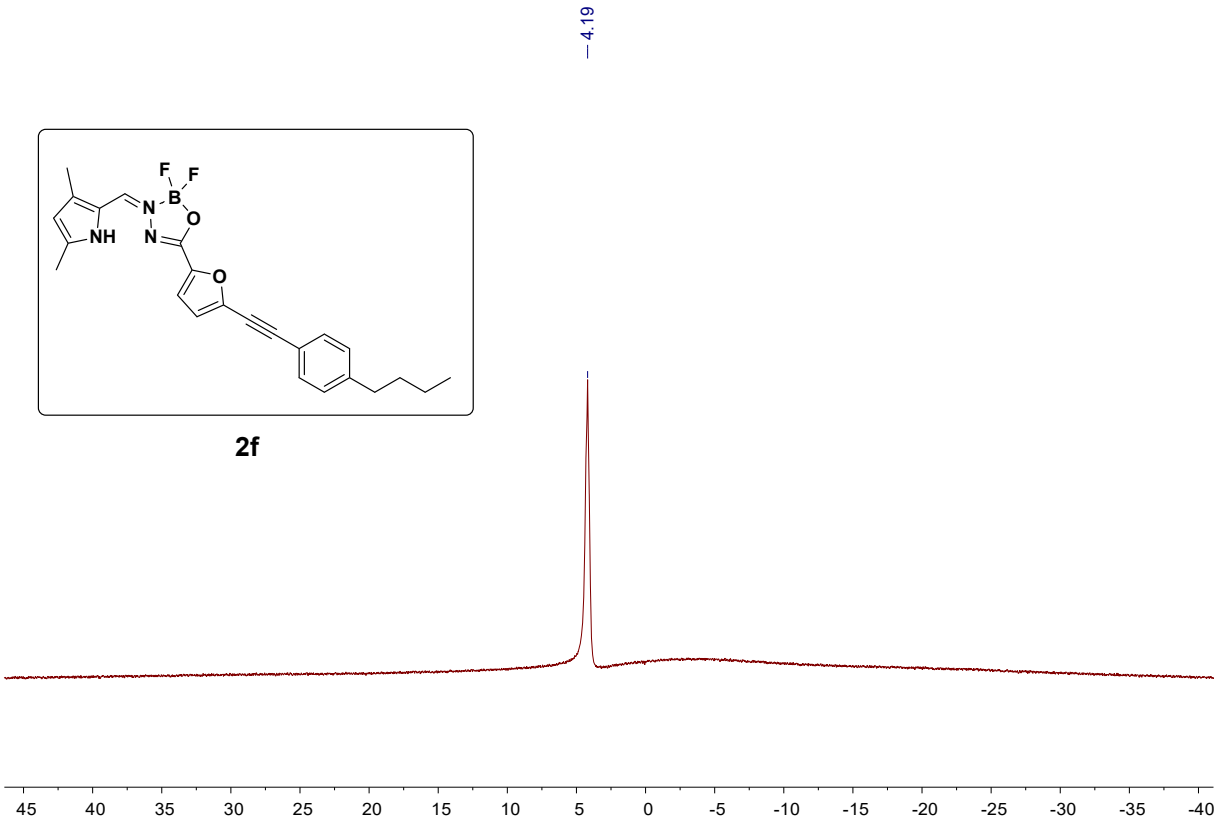

^{19}F NMR spectrum of 2f

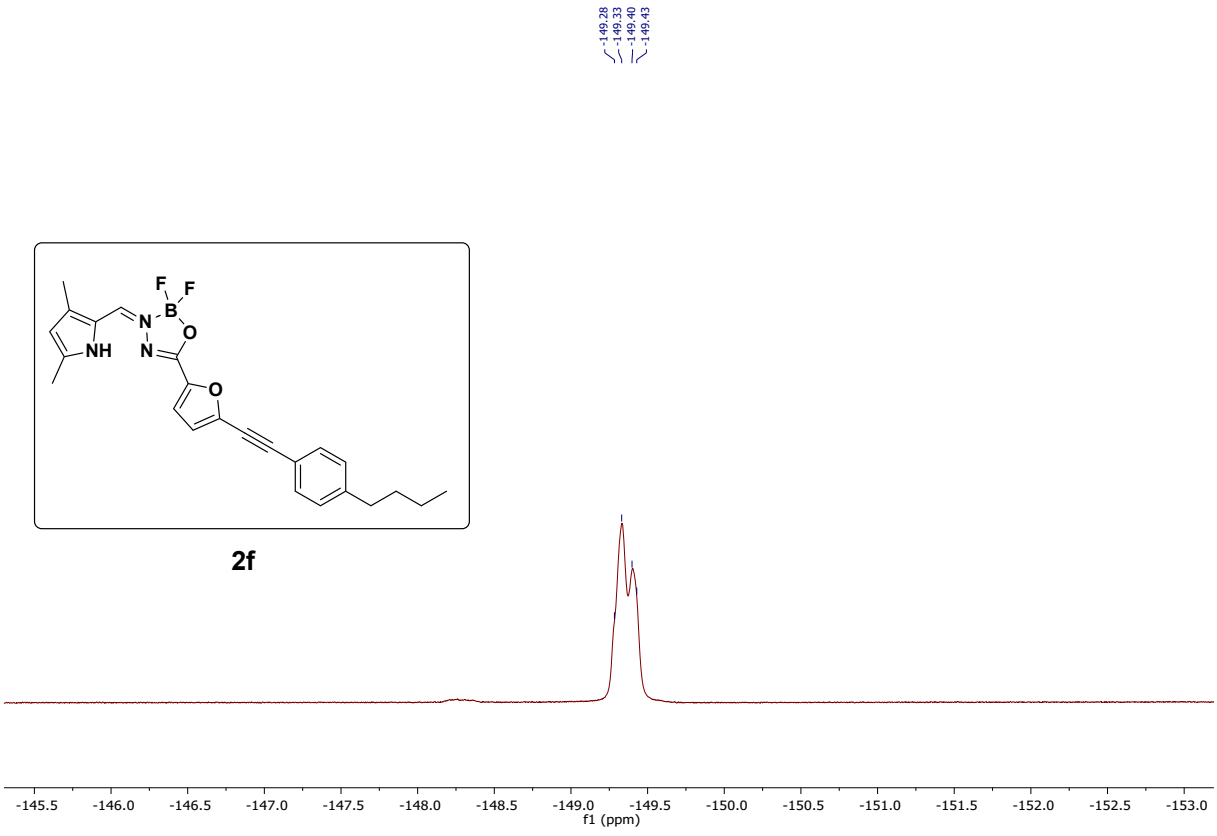

^{1}H NMR spectrum of 2g

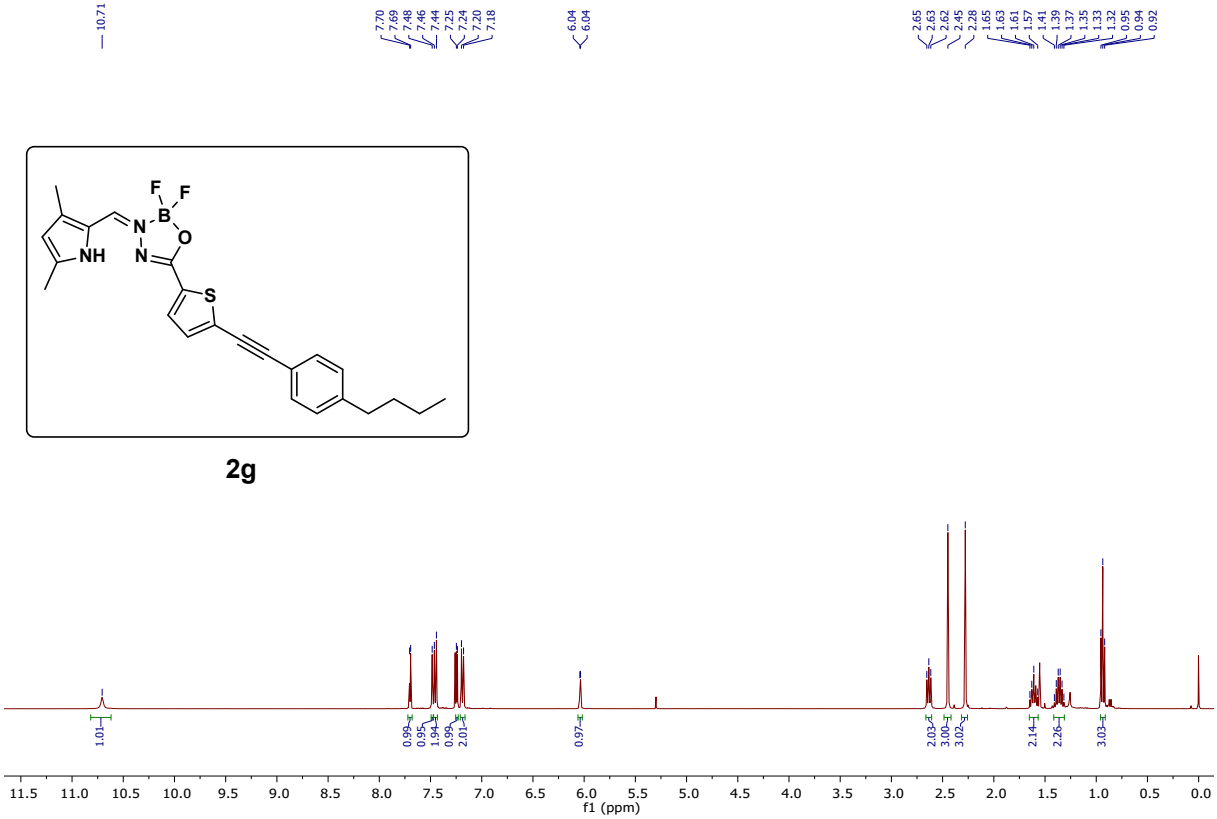

^{13}C NMR spectrum of 2g

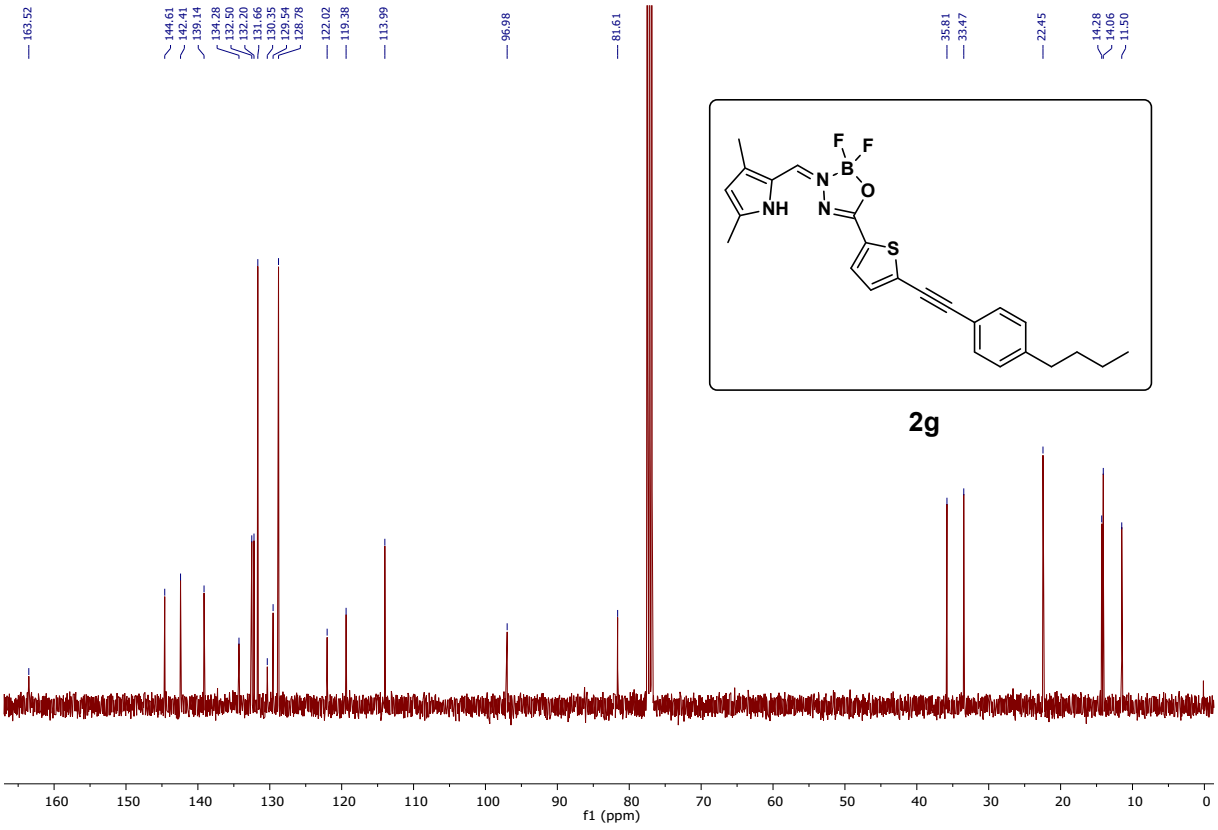

^{11}B NMR spectrum of 2g

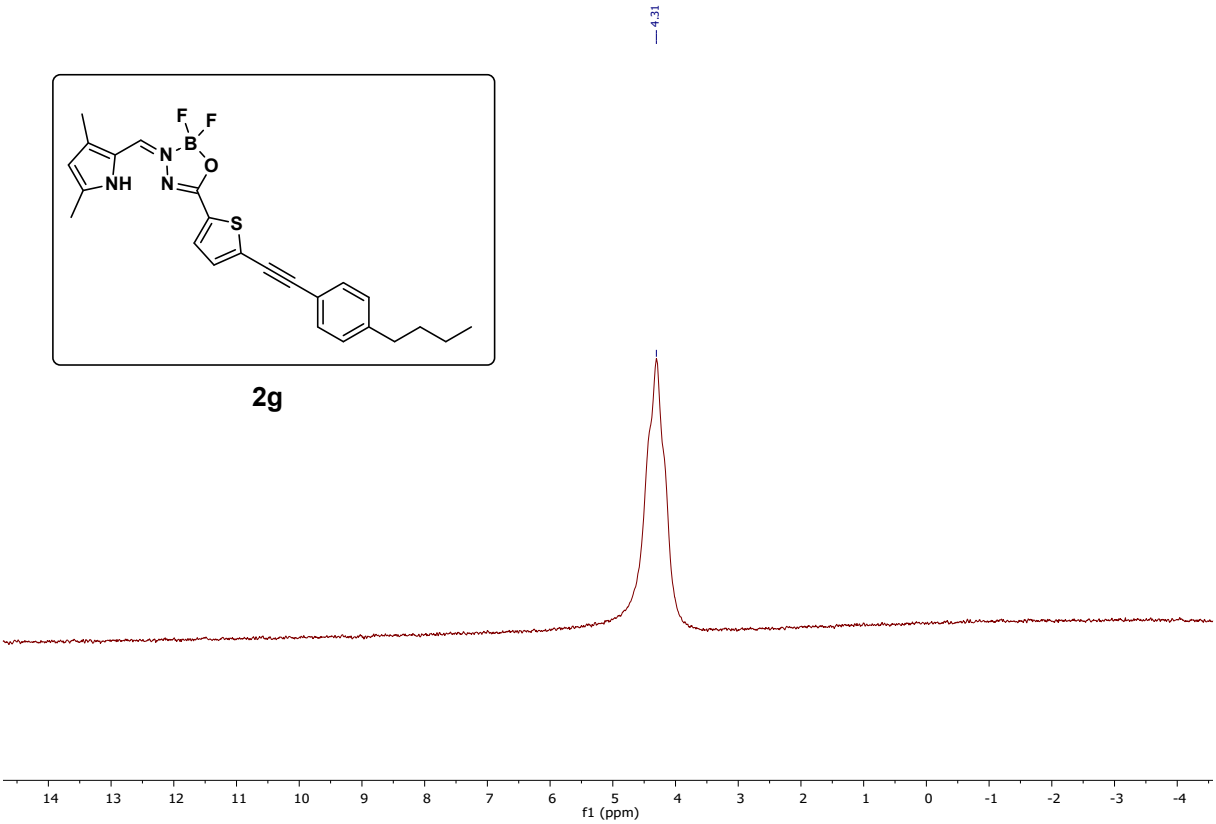

^{19}F NMR spectrum of 2g

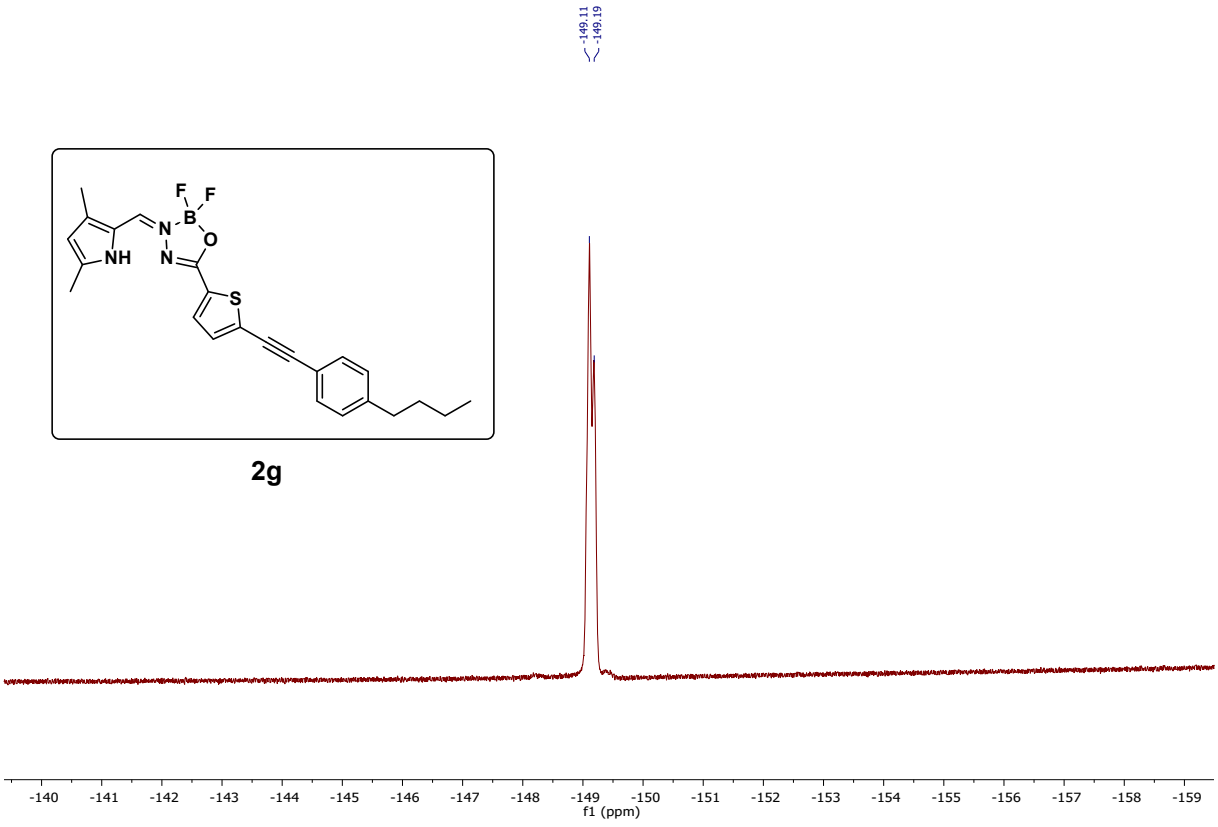

References

1 Rigaku OD, 2018.
2 O. V Dolomanov, L. J. Bourhis, R. J. Gildea, J. A. K. Howard and H. Puschmann, *J. Appl. Crystallogr.*, 2009, **42**, 339–341.
3 G. M. Sheldrick, *Acta Crystallogr. A*, 2015, **71**, 3–8.
4 G. M. Sheldrick, *Acta Crystallogr. C*, 2015, **71**, 3–8.
5 M. Singh, K. McKenzie and X. Ma, *J. Biotech Res.*, 2017, 78–82.
6 M. D. Abràmoff, P. J. Magalhães and S. J. Ram, *Biophotonics Int.*, 2004, **11**, 36–42.
7 C. A. Schneider, W. S. Rasband and K. W. Eliceiri, *Nat. Methods*, 2012, **9**, 671–675.